(2)

Report No. CG-D-11-90

THE DEVELOPMENT OF A CHARGE ALGORITHM FOR THE OPTIMIZED CHARGING OF A 120 V FLOODED LEAD-ACID LIGHTHOUSE BATTERY WITH FORCED ELECTROLYTE DESTRATIFICATION

Prepared by:

DIETER NOWAK, PH.D.

Electrochemical Energy Storage and Electric
Propulsion Laboratory
of the
Johnson Research Center
University of Alabama in Huntsville

FINAL REPORT
OCTOBER 1989

Prepared for:

U.S. Coast Guard
Research and Development Center
Avery Point
Groton, Connecticut 06340-6096

and

U.S. Department Of Transportation
United States Coast Guard
Office of Engineering, Logistics, and Development
Washington, DC 20593-0001

NOTICE

This document is disseminated under the sponsorship of the Department of Transportation in the interest of information exchange. The United States Government assumes no liability for its contents or use thereof.

The United States Government does not endorse products or manufacturers. Trade or manufacturers' names appear herein solely because they are considered essential to the object of this report.

The contents of this report reflect the views of the Coast Guard Research and Development Center, which is responsible for the facts and accuracy of data presented. This report does not constitute a standard, specification, or regulation.

SAMUEL F. POWEL, III
Technical Director
U.S. Coast Guard Research and Development Center
Avery Point, Groton, Connecticut 06340-6096

Technical Report Documentation Page

1. Report No.	2. Government Accession No.	3. Recipient's Catalog No.
CG-D-11-90		

4. Title and Subtitle	5. Report Date
THE DEVELOPMENT OF A CHARGE ALGORITHM FOR THE OPTIMIZED CHARGING OF A 120 V FLOODED LEAD-ACID LIGHTHOUSE BATTERY WITH FORCED ELECTROLYTE DESTRATIFICATION	OCTOBER 1989
	6. Performing Organization Code
7. Author(s)	8. Performing Organization Report No.
Dieter Nowak, Ph.D.	R&DC 09/88
9. Performing Organization Name and Address	10. Work Unit No. (TRAIS)
Electrochemical Energy Storage and Electric Propulsion Laboratory of the Johnson Research Center University of Alabama in Huntsville	11. Contract or Grant No. MIPR Z51100-6-00002
12. Sponsoring Agency Name and Address U.S. Coast Guard Research and Development Center Avery Point Groton, Connecticut 06340-6096 Department of Transportation U.S. Coast Guard Office of Engineering, Logistics, and Development Washington, D.C. 20593	13. Type of Report and Period Covered FINAL
	14. Sponsoring Agency Code

15. Supplementary Notes

16. Abstract

Proper charging was identified as the most important requirement for the reliable and economical operation of a battery that is part of the hybrid power system for remote lighthouses. Therefore a charge algorithm was developed to optimize charging of a flooded lead-acid battery with forced electrolyte destratification. This algorithm is independent of the operating temperature, the state of charge and the battery age. It controls charging according to the weakest battery module in the pack and is able in the course of several cycles to automatically equalize the performance of the modules in the battery pack without excessive overcharging. The charge algorithm prevents overheating due to bad battery connectors and quite generally responds to all causes of poor charge acceptance with a gentle treatment of the battery during charging.

Keywords: ELECTRIC BATTERIES; LIGHTHOUSES; LEAD ACID BATTERIES (RH)

17. Key Words		18. Distribution Statement
Battery Charging Charge Algorithm Cycle-Charged Diesel Hybrid Powers	Remote Power Aids to Navigation Lighthouses	Document is available to the U.S. public through the National Technical Information Service, Springfield, Virginia 22161

19. Security Classif. (of this report)	20. SECURITY CLASSIF. (of this page)	21. No. of Pages	22. Price
UNCLASSIFIED	UNCLASSIFIED		

Form DOT F 1700.7 (8/72) Reproduction of form and completed page is authorized

METRIC CONVERSION FACTORS

Approximate Conversions to Metric Measures

Symbol	When You Know	Multiply By	To Find	Symbol
		LENGTH		
in	inches	* 2.5	centimeters	cm
ft	feet	30	centimeters	cm
yd	yards	0.9	meters	m
mi	miles	1.6	kilometers	km
		AREA		
in^2	square inches	6.5	square centimeters	cm^2
ft^2	square feet	0.09	square meters	m^2
yd^2	square yards	0.8	square meters	m^2
mi^2	square miles	2.6	square kilometers	km^2
	acres	0.4	hectares	ha
		MASS (WEIGHT)		
oz	ounces	28	grams	g
lb	pounds	0.45	kilograms	kg
	short tons (2000 lb)	0.9	tonnes	t
		VOLUME		
tsp	teaspoons	5	milliliters	ml
tbsp	tablespoons	15	milliliters	ml
fl oz	fluid ounces	30	milliliters	ml
c	cups	0.24	liters	l
pt	pints	0.47	liters	l
qt	quarts	0.95	liters	l
gal	gallons	3.8	liters	l
ft^3	cubic feet	0.03	cubic meters	m^3
yd^3	cubic yards	0.76	cubic meters	m^3
		TEMPERATURE (EXACT)		
°F	Fahrenheit temperature	5/9 (after subtracting 32)	Celsius temperature	°C

* 1 in = 2.54 (exactly) For other exact conversions and more detailed tables, see NBS Misc. Publ. 286, Units of Weights and Measures. Price $2.25. SD Catalog No. C13.10:286

Approximate Conversions from Metric Measures

Symbol	When You Know	Multiply By	To Find	Symbol
		LENGTH		
mm	millimeters	0.04	inches	in
cm	centimeters	0.4	inches	in
m	meters	3.3	feet	ft
m	meters	1.1	yards	yd
km	kilometers	0.6	miles	mi
		AREA		
cm^2	square centimeters	0.16	square inches	in^2
m^2	square meters	1.2	square yards	yd^2
km^2	square kilometers	0.4	square miles	mi^2
ha	hectares (10,000 m^2)	2.5	acres	
		MASS (WEIGHT)		
g	grams	0.035	ounces	oz
kg	kilograms	2.2	pounds	lb
t	tonnes (1000 kg)	1.1	short tons	
		VOLUME		
ml	milliliters	0.03	fluid ounces	fl oz
l	liters	0.125	cups	c
l	liters	2.1	pints	pt
l	liters	1.06	quarts	qt
l	liters	0.26	gallons	gal
m^3	cubic meters	35	cubic feet	ft^3
m^3	cubic meters	1.3	cubic yards	yd^3
		TEMPERATURE (EXACT)		
°C	Celsius temperature	9/5 (then add 32)	Fahrenheit temperature	°F

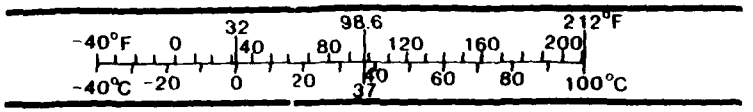

TABLE OF CONTENTS

LIST OF ILLUSTRATIONS

LIST OF TABLES

ACKNOWLEDGEMENT

This work was sponsored by the U.S. Coast Guard Research and Development Center as part of a project to develop a fully automatic hybrid power system for remote lighthouses.

The following persons are recognized for their contribution to the success of this project:

Jeff Sinex of the EEPL for conducting all tests and for translating the charge algorithm into computer code. He contributed Section 3.5.2 and the Appendix 2 to this report.

LeRoy Slater of the EEPL for the preparation of the test rigs and their instrumentation.

Johannes Meiwes of the EEPL for contributing his ideas during dicussions in which various aspects of the test results were analyzed.

Tony Barrett for his cooperation and help in the installation of the hybrid power system at UAH.

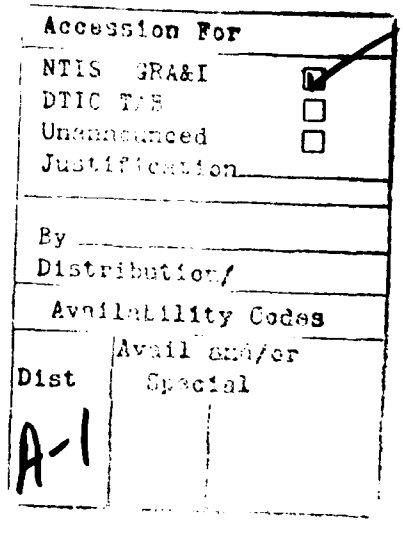

[BLANK]

THE DEVELOPMENT OF A CHARGE ALGORITHM FOR THE OPTIMIZED CHARGING OF A 120V FLOODED LEAD-ACID LIGHTHOUSE BATTERY WITH FORCED ELECTROLYTE DESTRATIFICATION

1.0 INTRODUCTION

The Electrochemical Energy Storage and Electric Propulsion Laboratory (EEPL) of the University of Alabama in Huntsvillle (UAH) is under contract to the U.S. Coast Guard to develop a battery-based energy system with an optimized charge algorithm for application in remote lighthouses. The energy system is a hybrid, multi-energy source system, but the prime source is a diesel generator with a 120 volt storage battery. This is the final report of Task 2 of the total effort: the development and implementation of a charge algorithm, that maximizes energy efficiency by minimizing diesel run time. It optimizes battery performance and battery life by optimizing the overcharge factor of the battery and by charging the battery with a current corresponding to the maximum charge acceptance of the weakest module in the battery pack. The results of other parts of the total effort are described in separate reports.

At the present time, power for lighthouses that have no commercial powerline connection is supplied by diesel generators which run 24 hours per day. This type of lighthouse operation requires frequent and costly diesel generator maintenance and lower power source reliability than desired by the U.S. Coast Guard. Moreover, since the diesel motor has to supply the whole spectrum of power needs of the lighthouse, from very low electrical loads to peak loads, the installed diesel power plant is oversized for the mostly low average power. Therefore,

the diesel runs substantially throttled for long periods of time which increases the wear on the motor and causes inefficient utilization of fuel.

If the diesel generator is only used to charge the battery and the battery is used as the continuous source of power for the lighthouse, then the diesel generator can run at a much higher efficiency at a more optimum output power and it will run for a much shorter period of time. Since a low discharge rate is a favorable operating mode for the battery, and if that is sufficient to power the lighthouse, and the fact that the higher output power is a more favorable operating mode for the diesel generator makes the combination represent an ideal set of conditions for the system.

In summary, the beneficial effect of the battery with respect to the hybrid power system for lighthouses stems from the capability of the battery to accept charge at a high rate and to give it off efficiently at a low rate. But if a battery is to be an economical and reliable energy storage system for remote lighthouses, a number of requirements have to be satisfied by the battery, the most important of which are listed below. They are:

a) Long battery life to justify the high initial cost for the battery and to provide reliable power system operation.

b) Optimized maximum charging rates to minimize diesel running time to reduce fuel, maintenance and wearout costs of the system.

c) Long intervals between battery maintenance cycles to minimize the operating cost of the system. One objective of the hybrid power system is a one year time period between maintenance cycles.

The selection of a suitable battery is the most important step for satisfying these requirements. But once the battery has been selected then these requirements can best be satisfied by proper charging. The development of a proper charging algorithm for the Hagen battery delivered by the EEPL to the U.S. Coast Guard is the subject of this report.

The charge algorithm decribed in Section 3 is based on the UAH charge algorithm described in Section 2. The UAH algorithm was previously developed under contract to The Aerospace Corporation for the U.S. Department of Energy [1]. The algorithm concerns the charging of high voltage conventional flooded lead-acid battery packs made up of modules such as the Alco 2200 golf cart battery. It needs a gas rate sensor as a control signal device to charge the battery along its charge acceptance curve [F1]. The algorithm is essentially self compensating for battery temperature, battery age and state of charge over a wide range of these parameters.

The first generation, Aerospace/DOE/UAH algorithm works very well for flooded lead-acid batteries with static electrolyte, but it is difficult to apply to batteries with forced electrolyte destratification provided by mechanical pumps to circulate the electrolyte, such as the Hagen battery system currently under test by the U.S. Coast Guard. The first generation algorithm relies on the gas rate measurement of only one module to control the charge for all modules in the pack. This can cause over- or undercharging of other modules

---

F1 Basically two electrochemical reactions take place in the battery: the charge reaction and the gassing reaction (electrolysis). Charge acceptance describes the quantity of current consumed in the charge reaction. This is discussed in Section 2.

in the battery pack, if the battery module being monitored is not representative of the other modules. Therefore, based on work done for other projects [2], the EEPL developed for the Hagen battery system a gas controlled charge algorithm that does not need gas sensors. This algorithm was verified in tests using a 120 Volt and a 144 Volt Hagen battery system, which were built and modified at the EEPL as part of Task 1 of the total effort. A laboratory power supply and a HP data aquisition and control system was used as a charger in these tests.

Subsequently, a full-fledged lighthouse power system was built at the EEPL consisting of a Lister diesel generator and its controller. Then the new charge algorithm was tested with the lighthouse power system. After successful completion of the test, the charge controller and its software were shipped to the U.S. Coast Guard Development Center in Groton, CT for further testing with their lighthouse prototype.

This report includes a discussion of why the development of a complex charge algorithm is needed to minimize the running time of the lighthouse diesel generator to obtain the objective of the total effort: The development of a hybrid power system that has maintenance intervals of not less than one year. Further, the report explains how and why the algorithm works and what effects on the battery it has. To this end a summarized background on facts relating to charging and pertinent to the development of the charge algorithm is provided in Section 2. Section 3 is a description of the charge algorithm, its implementation in the hybrid power system and its effect on battery behavior under special conditions such as an unbalanced battery pack. Section 4 is a Summary.

2.0 BACKGROUND

It was stated in the introduction that the beneficial effect of the hybrid power system for remote lighthouses stems from the capability of the battery to accept electric energy at a high rate during charging and to give it off efficiently at a low rate during discharging. The following Section 2.1 discusses the role of charge acceptance [F3] in the design of an optimum charge algorithm. In subequent sections, it will be shown that charge acceptance can be determined by a gas rate measurement in the cells and that optimized charging is achieved by controlling the gas development in the cells. After a discussion of the selection of a proper gas rate limit, the gas controlled UAH algorithm is described that is the forerunner of the newly developed algorithm for the hybrid power system.

2.1 The Charge Acceptance as Central Problem of Optimized Charging

Since the diesel motors installed in remote lighthouses around the U.S. are capable of generating power far in excess of what is needed to supply electricity to the lighthouses, it would be advantageous to select batteries with a capability to accept a very high rate of charge (large charge acceptance) to make use of the excess power. Since the voltage of the lighthouse system is limited to 120 volts, a high charge acceptance can best be achieved by batteries with a large capacity, i.e. large industrial batteries.

F3. Charge acceptance is defined as the ratio $(I - I_{EL})/I$ where I is the charge current and I_{EL} is the current used for electrolysis of the electrolyte. It indicates how much charge is stored at any time during charging and how much is lost to electrolysis. (See also Section 2.2)

The operating conditions using such large batteries would be ideal for diesel generator charging if the battery was able to accept charge at a constant high rate until the fully charged state is reached. Unfortunately, no battery is able to do that no matter how big its capacity. Instead, the nature of electrochemical processes causes a continuous decline in the amount of power that can be converted to charge the battery as the state of charge of the battery nears the end of charging. In the end, even large batteries can accept only a trickle charge current. Excess current is used up in electrochemical processes other than charging that are invariably harmful to the battery.

Short of ideal operating conditions for the diesel motor, the best charge is the one that supplies energy at the maximum rate at which the battery can accept. This will maximize battery life, capacity and efficiency and generate the least amount of water losses in the electrolyte. If less power is supplied, then the charging process takes longer, thus increasing diesel running time. If more power is supplied, then the excess power is primarily used for electrolysis which produces hydrogen and oxygen from the water in the electrolyte. This dries out the battery, thus requiring more frequent battery maintenance in the form of water replenishment and also reduces battery life.

The central question for optimum charging then is: What is the maximum rate of energy [F4] that the battery will accept for storage at any time during the charging process at any state of charge?

F4. Current and voltage of a battery are not independent parameters. If a voltage is imposed on the battery by an external source, then the battery will respond with a current that depends on the state of charge. If a current is forced into the battery, then the battery voltage will rise to levels that depend on the state of charge. Hence if current is controlled, then maximum energy acceptance for charging corresponds to the maximum current acceptance for charging.

The solution to this problem is given in the form of a charge algorithm that controls the current output of the diesel generator to the level of energy the battery is capable of storing. The algorithm is discussed in Section 3.0. As will be realized, the algorithm is very complex. The complexity of the charge algorithm is caused by the need for a control loop with a complex feedback. Since the development of charge acceptance during charging is not only a function of the state of charge of the batte:)ut also depends on battery temperature, battery age, electrode design and the immediate history of cycling which the battery went through, the charge acceptance is not predictable with enough accuracy to optimize the charging process. Therefore, an appropriate sensor is needed that provides a steady flow of information during charging on the status of charge acceptance to the charge controller which then adjusts the current output to the battery accordingly.

The problem of finding an appropriate charge acceptance sensor is exacerbated by the difference of charge acceptance of the cells in a high voltage battery pack that are exposed to the same charge current. To prevent overcharging of any of the cells in the battery pack, the charge acceptance of each cell must be monitored individually and the charge current must be regulated according to the need of the cell with lowest charge acceptance. The charging problem can therefore be divided into two parts: (1) how to measure charge acceptance continuously during charging and (2) how to find the cell with the lowest charge acceptance in the high voltage battery in a practical manner,i.e. with an effort that can be tolerated in field operation of the battery from an economical point of view. These questions are addressed in the sections below.

2.2 The Determination of Charge Acceptance

The charging process of a lead-acid battery is the conversion of lead ions of valance 2 to lead ions of valence 4 at the positive electrode while giving off electrons, and the conversion of lead ions of valence 2 to metallic lead under consumption of electrons.

The Pb^{2+} is not soluble in the electrolyte and is therefore available only as part of the $PbSO_4$ in the crystals of the discharged electrodes. These crystals are dissolved during charging.

Positive electrode	$Pb^{2+} \rightarrow Pb^{4} + 2e^{-}$
Negative electrode	$Pb^{2+} + 2e^{-} \rightarrow Pb$

To measure the charge acceptance directly means to measure the Pb^{2+} consumption at each electrode and to compare it with the amount that would result if the charge current was completely used for the charge reaction, according to the Faraday Law that governs electrochemical processes. This is not possible because the charge reaction takes place at the interface between electrolyte and electrode surface which is inaccessible for measurement during battery cycling.

Therefore efforts to measure charge acceptance must be directed toward measuring charge acceptance indirectly. The logical way to approach this problem is to look for effects outside the battery that can be measured. In this respect a convenient way to measure charge acceptance is to measure the gas rate of the gas generated in the battery cells. Although the charging process is accompanied by a combination of other electrochemical processes such as electrolysis and electroplating and corrosion of the electrode grids and cell

conductors, the charge reaction and the electrolysis are the only processes that have measureable effects during any one charge. All other processes will show effects only in the course of many cycles and can therefore be neglected during any one cycle. Therefore, if the gas rate is known during charging, then the amount of current used for the gassing reaction can be calculated, assuming stoichiometric gas relationships of H_2 and O_2, and the difference between the current delivered by the charger and the current used for gassing is the current accepted for the charge reaction.

There are limitation w.r.t. accuracy to determining charge acceptance through gas rate measurements alone. Both the charging reaction and the gassing reaction through the electrolysis share in the amount of current which passes through the battery. The fact that both electrochemical reactions are present simultaneously at eacn electrode results in nonstoichiometric quantities of hydrogen and oxygen at each electrode: to satisfy current continuity requires only that current consumption of electrolysis and charge reaction combined is the same at each electrode. How much current goes into electrolysis and how much into charging can be different for each electrode at any time during charging. Only when the battery is about 95% fully charged, i.e. toward the end of charging, approaches the relationship of the oxygen and hydrogen gas quantities stoichiometric conditions. This in effect is to say that the charge acceptance of the positive and negative electrode is different from each other throughout most of the charge time and to determine the charge acceptance of the electrodes, the percentage of H_2 and O_2 in the gas must be measured too. Only at the beginning of charging of a discharged battery when the gassing process is absent and at the end of charging when all current is used for electrolysis is

the charge acceptance of both electrodes the same. The charge acceptance of the cell is defined as the sum of the charge acceptance of both electrodes. Because current consumption for equal volumes of oxygen and hydrogen gas differs, the determination of charge acceptance by assuming stoichiometric gas relationship contains an error. However, this error is insignificant for gas controlled charging since the gas is anyway controlled only within a predefined range and very accurate values for charge acceptance are not required.

Since it is now clear that minimizing the gas production in the battery cells during charging results in charging along maximum charge acceptance the question on how to achieve this is now addressed. Also discussed is why charging with zero gas production is not possible even though sealed batteries such as lead-acid battteries with gelled electrolyte seem to indicate otherwise. To this end the current-voltage relationship during charging are discussed in the next section.

2.3 Optimized Charging Through Gas Control

Although the parameter determining the quantity of conversion involved in each electrochemical process is the charge current, it is the charge voltage that determines the onset of the electrochemical reaction. The theoretical voltage to initiate gassing (electrolysis of water) is 1.23 V. In contrast, the theoretical voltage required to initiate charging is much higher. (>1.8V) It is also variable, lower for a discharged battery and higher towards the end of charging. Therefore the lead-acid battery would not work if both electrochemical processes would be initiated at the theoretical voltages. The electrolyte would be transformed to hydrogen and oxygen before the charging process could

begin. The lead-acid battery works because the real process of electrolysis has to overcome a higher electrical resistance, apparent as overvoltage, than the charging process. The overvoltage is the actual voltage required to initiate the electrochemical process minus the theoretically required voltage.

As the battery nears the fully charged state, the electric resistance to charging increases while the electric resistance to electrolysis stays essentially the same. The reason for the increase of electric resistance during charging is that Pb^{2+} ions must be transported by diffusion to the surface of the electrodes. As the reservoir of $PbSO_4$ at the electrodes decreases with increasing state of charge, the charge reaction at the electrolyte-electrode interface lacks sufficient quantities of reactants and the path of transportation for the reactants becomes larger and larger. At some state of charge even very high overvoltages will not be able to induce more current consumption for charging beyond a current limit. This is seen in Figure 1.

Each solid curve in Figure 1 indicates the current-voltage relationship during charging at a particular state of charge. The point-dashed line is the current-voltage relationship of the gassing process (electrolysis). It is independent of the state of charge. During the latter part of the charge both the gassing reaction and the charging reaction have a major impact on the current-voltage relationship during charging. How this relationship would look like without gassing reaction is indicated by the dashed curve continuation which represents the current-voltage relationship of the charge reaction alone.

Curves such as shown in Figure 1 are obtained by increasing the charge current through the cells in steps and measuring the cell voltage response, the

gas rate and the gas constituents. Using the Faraday equivalent, the currents needed to generate the measured amount of hydrogen and oxygen can then be calculated and added to obtain the total gassing current. For corresponding voltages the gassing current has to be deducted from the total current through the cell to arrive at the current values for charging and to obtain the corresponding current-voltage curves for the charging process that are indicated in Figure 1. The current-voltage relationship for gassing is obtained by plotting voltage over gassing current.

To understand this procedure one must note that current conduction through the electrolyte is facilitated by two streams of ions, one being negatively charged, the other being positively charged. These streams move in opposite directions to the corresponding electrodes and are then neutralized there by taking on or giving off electrons. Further current conduction through the active material and the electrode grids is by electron conduction. The total current through the cell is the sum of charges per unit time contained in both ion flows. Therefore, the hydrogen generation during the gassing phase of charging at the negative electrode is generated by a current in the negative direction, while oxygen is produced at the positive electrode by a current in the positive direction. The current available for charging is reduced by the sum of oxygen and hydrogen current because the total supply of ions available for charging is reduced by the amount of ions involved in the charge transport for both gassing reactions.

Figure 1 indicates that at the beginning of charging a discharged battery, the voltage required to initiate the charging process is low. Moreover, the battery is able to accept large amounts of current without reaching the state of

heavy gassing. A small increase in charge voltage results in large increases in current. Of course, a proportional part of this energy is used up for heat generation so that it is an accepted rule of thumb not to increase the charge current beyond the five hour rate [F5] to prevent damage of the battery from overheating.

As the battery state of charge increases, the voltage needed to initiate the charging process is growing. This is seen in Figure 1 by the shift of the origin of the initial current-voltage relationship of the charging process towards the right for an increase in the state of charge. Meanwhile the voltage needed to initiate gassing stays essentially the same. Since gassing starts at 1.23 V it is seen that the battery must be allowed to produce a limited amount of gas in order to become fully charged, i.e. reach the charge reaction curve to the far right (G in Figure 1). Thus the battery cannot be charged completely free of gassing.

Let us now turn to curve F in Figure 1. As seen for U_2, a reduction in voltage decreases both the charging current and the current for the gas production. Likewise a reduction of total current reduces the charge voltage, the gassing current, i.e. the gas rate, and the charge current. Because the gradient of the current-voltage relationship of the gassing reaction is much larger than that of the charging reaction, the reduction in charge current reduces the gassing current more than the current of the charge reaction. Thus the gas rate at any time during charging can be reduced by reducing the charge voltage or the

---

F5. The 5 hour rate is the current at which the battery will discharge 80% of the capacity within 5 hours.

charge current. Current control is preferable in particular for multi-cell battery packs for two reasons: (1) the current gas rate relatinship is not as sensitive to changes in current as the voltage-gas rate relationship is to changes in voltage. Control is thus easier. (2) The voltage control uses the total voltage as control feedback to the charger. If the total voltage is held at any one level, then the individual cell voltages are free to move to any level consistent with the state of charge of the cell, as long as the sum of all cell voltages adds up to the control voltage. Thus, in an unbalanced battery pack [F6] some cells might never reach the maximum end-of-charge voltage and become permanently undercharged. This results in electrode sulfation and short battery life. If, however, the charge is current controlled then electrochemical reactions, either charging or electrolysis, must occur in all cells as long as the current flows through the battery. Therefore if the current is kept low enough to prevent excessive gassing in any of the cells, then they can be prevented from undercharging as well as overcharging.

We now have all the elements for the optimized charge algorithm together that has been realized in the UAH charge algorithm: At the beginning of charging a fully discharged battery the current is held constant at the five hour rate until gassing sets in. Then the battery is charged at the rate of maximum charge acceptance by controlling the gassing rate which in turn is controlled by regulating the current.

F6. An unbalanced battery pack consists of cells that are at different state of charges.

2.4 Determination of Permissible Gassing Rates for Charging

It has been stated that gassing of a battery cannot be completly eliminated if the battery is to be fully charged. Hence, the question arises what the required level of gassing is that must be permitted. To determine the answer to this question another aspect of gassing must be considered. It is the stratification of the electrolyte.

The electrochemical charging process of the lead-acid battery involves the electrolyte as partner in the reaction. Consequently the density of the electrolyte changes significantly during charging and discharging unless a large electrolyte reservoir is available. This density change results in convective fluid flow between the electrodes if sufficient space is available for the electrolyte to move. The convective flow causes some equalization between electrodes in particular if the plates are of a tubular design. Towards the bottom of the cell, however, very little equalization occurs. Since stratification for a number of reasons is very harmful to battery life and impedes battery performance, an artificial equalization process is highly desirable.

The most common equalization process is that through deliberate gassing in the cells. Although gassing itself is harmful to the battery as mentioned earlier, it is generally agreed that heavy stratification is even worse. The commonly accepted strategy during charging is therefore to allow an increased amount of gassing over what is nessessary to fully charge the battery during the current taper phase [F7] of the charge to achieve equalized specific gravity at

---

F7. Since the charge acceptance decreases toward the end of charging the charge current has to taper down to avoid heavy gassing. This charge phase is called "taper phase".

the bottom and top of the cell at the end of charge. The development of specific gravity for such a charge is seen in Figure 2. Since the amount of gassing needed to destratify the electrolyte is greater than the amount generated to fully charge the battery, destratification through gassing defines the gas rate limit in gas controlled charging. At the EEPL tests have been conducted to determine the optimum gas rate for destratification. It was found that about 30-40 ml/min/cell constant gassing rate from the time when the battery begins noticeably gassing to the end of charge gives the best results for tubular batteries such as the Hagen battery used in the Coast Guard project.

What has been discussed so far represents the background for the UAH charge algorithm that has been developed by the EEPL for gas controlled charging of conventional lead-acid batteries. Since the charge algorithm developed for the U.S. Coast Guard is based on it, the UAH algorithm is discussed in the next section.

2.5 The UAH Algorithm For Gas Controlled Charging

The key hardware elements for the UAH charge algorithm are a gas rate sensor and a microprocessor controlled power supply. The gas rate sensor measures the gas rate of 3 cells and takes this measurement as representative for the gas development of the whole battery pack. Each control step regulates the current to a particular level at which the current is held constant until another control step occurs.

Thus the charge is completely current controlled. It starts with a 5 A constant current charge for 2½ minutes to give the gas time to develop if the battery is already charged. In this case, it was found, the battery will

quickly begin to gas and if 34 ml/min/cell are reached during these 2½ minutes then the charger logic recognizes this as a charged battery and terminates the charge. If no shutoff occurs, then the current is stepped up by 5 A and held at 10 A for 2½ more minutes. The battery might not accept 10 A at very low temperatures and start to gas. If sufficient gas is generated to drive the gassing rate above a battery type dependent limit that is programmed into the charger, then the current is reduced by 0.3 A and held constant again. This causes at first a gas rate reduction to below the gas rate limit due to the reduction in current available for electrolysis. However, as the charge acceptance decreases, with progressing state of charge, more current becomes available for electrolysis and so the gas rate rises again. As the gas rate reaches the upper limit the current is again reduced. This procedure is reflected by a sequence of peaks and valleys in the gas rate versus time curve as the gas rate oscillates between a maximum set by the gas rate limit and a minimum set by the 0.3 A current reduction. These valleys in the gassing curve get longer and longer as charging nears completion because the charge acceptance drops asympotically to zero. Finally a point is reached where almost all current is used for electrolysis because the battery is fully charged. Therefore no additional current becomes available since the current is held constant. The gassing rate does not reach the gas rate limit any more and this condition is defined as the end of charge because it signals zero charge acceptance. In practial terms: If the gassing rate keeps below the gassing rate limit for 45 minutes then charging is terminated.

At temperatures and states of charge where the gas rate limit is not reached at 10 A the charge current is stepped up in steps of 5 A every 2½

minutes up to the 5 hour rate. This current is held constant until the gassing limit is reached. Then the current is stepped down in steps of 0.3 A each time the gassing limit is reached as stated before. One can see the current steps and the gas development in Figure 3.

Although this charge algorithm works very well, it has three major drawbacks: (1) It needs an expensive flow meter (2) It does not account for the differences in the charge acceptance from one cell to another of a high voltage battery pack unless the gas rate of each individual cell or module is measured which is impractical. In an unbalanced battery pack, this could cause undercharging of some cells while at the same time other cells are overcharged, thus causing battery damage. (3) The algorithm is hard to apply to a battery such as the Hagen battery used in this project the electrolyte of which is destratified by air lift pumps. This is because air is pumped into the cells as medium to move the electrolyte and this air cannot be separated from the gas developed during charging so that the determination of the gassing rate becomes quite complex.

The charge algorithm developed and applied as part of the hybrid power system project eliminates these draw backs of the UAH charge algorithm while maintaining its advantages. This is discussed in the next section.

3.0 A RESISTANCE CONTROLLED CHARGE ALGORITHM

Clearly the application of the UAH algorithm would be much easier if the gas rate sensor could be replaced by more inexpensive sensors with no need for plumbing. Current and voltage sensors have this quality. Voltage measurements can readily be obtained for each individual module of a battery pack with sensor wires attached to each positive post and a common ground, thus allowing to monitor the performance of all modules. Therefore, if a method could be found that in some way relates the gas control algorithm to module voltage and current measurements instead of module gas rate measurements, then the algorithm would not only be easier and more inexpensive to implement but could also be applied to batteries with forced electrolyte circulation and would be able to react to single module performance in its control response.

EEPL was able to find a relationship between current measurements and gassing rate that is satisfactory for charge control purposes. A charge control algorithm was designed around it that basically has the characteristic of gas controlled charging. The fundamental concepts used for this algorithm are discussed in the next sections. It will be shown that the rate of heat developed in the battery per $[A]^2$ increases with the state of charge and is especially steep when the battery begins to gas. Since heat rate, expressed as electric energy divided by the square of the charge current, can be interpreted as an electrical resistance, it will be shown how this resistance can be measured and consequently how gassing can be controlled by controlling the heat development through resistance control. To this end the determination of the heat development and its relationship to current and voltage are discussed first.

3.1 The Concept of Equilibrium Voltage, Overvoltage and Gassing Voltage.

The electric energy stored during charging is given by the product of charge quantity (number of electrons exchanged during the charge reaction) times the characteristic minimum voltage at which the charging reaction takes place. This product is the reversible part of the energy transfer during charging and is available for discharge. It is therefore the well known free reaction enthalpy which quantifies the reversible part of the reaction enthalpy of any chemical reaction.

Likewise, the electric energy stored as latent heat in the hydrogen and oxygen gas and recoverable when hydrogen is burned, is given by the product of charge quantity used in the gas reaction times a characteristic minimum voltage of the gassing process (electrolysis).

The characteristic minimum voltages of the electrochemical reactions are called "equilibrium" voltages. As the name "equilibrium" implies, the bulk quantities of the various reactants present in the equilibrium state do not change with time. However, the equilibrium is dynamic; changes take place at the local level. At the phase interface electrode-electrolyte there is a continuous interchanging of charged particles in both positive and negative directions causing corresponding electrochemical reactions in such a way that no electric current flows through the cells. Hence, for a disconnected battery all possible electrochemical processes, primarily charge reaction, discharge reaction, gassing and recombination reactions occur simultaneously but the system shows no trace of it to the surroundings.

If the battery terminals are disconnected from any load or charger then its voltage, the open voltage is very closely the equilibrium voltage of the

charge/discharge process. If the voltage on the battery is shifted to more positive values by a charger then the probability increases that more positive particles enter the electrolyte from the electrodes than are given up from the electrolyte to the electrodes and the battery is charged. For a differential shift in voltage the charge process would be free of losses except for the development of a small amount of heat as a consequence of the exothermic electrochemical charge reaction. The same reasoning applies to electrolysis. Gassing at equilibrium voltage would not generate heat.

In reality, the voltage shift needed to charge the battery at an acceptable rate is significant. The voltage difference between the charge voltage and the equilibrium voltage indicates an irreversible energy loss in the form of heat and is called the "overvoltage" during charging. As mentioned in Section 2, for a measurable amount of gassing, the overvoltage of the gassing reaction has to be higher than the overvoltage for the charge reaction. Since the battery voltage is generally much higher than the equilibrium voltage for gassing the heat production due to gassing is much higher than that due to charging if gassing current and charging current are of the same order of magnitude as is the case during the last phase of charging.

Because the equilibrium voltage for gassing is so much lower than that of charging, the charging and gassing reactions occur simultaneously throughout charging. However, until the charge voltage has reached a threshold of about 2.3 volts per cell, the charge acceptance of the battery is high and the gassing current very low so that the gassing quantities that are associated with lower charge voltages at the beginning of charging are so small that they are negligible for all practical purposes. This leads to the definition of a "gassing

voltage". The gassing voltage is arbitrarily set as the voltage at which the battery will develop measurable gas rates. It is a pivotal value for most charge algorithms. However for the algorithm described in subsequent sections it is not required explicitly.

The concept of equilibrium voltage and overvoltage are now used to develop a simplified mathematical model of the heat production in the battery. The model is needed to explain the charge algorithm.

3.2 A Simplified Model for the Heat Production in the Battery and its Relationship to Gassing.

It was mentioned in the previous section that energy losses in the battery are transformed into heat. If no heat losses would occur then the battery could be charged at the equilibrium voltage U_o corresponding to the state of charge of the battery, with the power

$$P_{CH} = 0.97U_o\ (I - I_{EL}) \qquad (1)$$

where I is equal to the charge current delivered by the charger and I_{EL} is equal to the current that is used up for gassing.

The factor 0.97 accounts for the fact that the charging reaction is exothermic (produces heat). This is felt as a lower voltage needed to charge the battery.

The equilibrium voltage depends on the concentration of the electrochemically active ingredients in the electrolyte which changes with the state of charge. The equilibrium voltage of the battery increases as the battery is fully charged. Figure 4 indicates the dependency of the equilibrium voltage

on the effective electrolyte density. The effective electrolyte density at a particular time during charging is the bulk density of the electrolyte in the battery cells. It is the average of all local densities in the pores of that part of the active material that is affected by the chemical changes of the charge reaction at that time.

It is seen from Figure 4 that even for a discharged battery the equilibrium voltage of the charge-discharge reaction is higher than 1.8 Volts. This compares to 1.23 Volts of the gassing reaction.

If no losses would occur during the electrolysis of the water in the electrolyte then the power used to electrolyze the water would be

$$P_E = I_{EL} \cdot U_{OE} \qquad (2)$$

where U_{OE} = 1.48V and is independent of the electrolyte concentration. This voltage is higher than the 1.23 volts theoretically needed for electrolysis, and accounts for the heat that is consumed during electrolysis thus requiring extra energy (voltage) to generate heat.

The power used to generate heat in the battery at a certain rate is the power from the charger U x I minus the power absorbed by the charge reaction minus the power absorbed by the electrolysis.

$$Q = UI - 0.97\ U_O\ (I - I_{EL}) - U_{OE}\ I_{EL} \qquad (3)$$

$$Q = (U - 0.97\ U_O)I + (0.97\ U_O - U_{OE})\ I_{EL} \qquad (4)$$

Equation (4) indicates how the heat generated in the battery relates to the overvoltage and the currents involved in the charging reaction and the gassing reaction. This relationship is the basis for the correlation of voltage and current measurements with gassing rate measurements that is discussed in the next section.

3.3 Correlation Between Electric Resistance and Heat Generation in the Battery.

As mentioned earlier, only 3% of the heat generated in the battery is caused by the charge reaction. Most of the heat development is the result of irreversible work needed to transport charged particles through the battery. Therefore, the generation of heat can be thought of as the result of the action of an apparent electrical resistance "R_i" in the battery. It must be overcome to transport the charged particles from one electrode surface to the other.

Hence R_i is defined such that

$$\dot{Q}(t) = R_i(t)I^2(t) \qquad (4a)$$

at any time during charging. Equation (4a) indicates the time dependency during charging of the parameters incolved in the equation. Of particular importance is the time dependency of R_i which is the cause of significant changes in the heat rate during charging even if the current is held constant. This is seen in Figure 5 for a conventional constant current - constant voltage - constant current charge, whereby the heat rate and the corresponding charge current are plotted into the same figure. Clearly, the heat rate is charactistic for each charge phase and if the heat rate is used as information for gas control, during

charging then it is of interest to know how much of the heating resistance stems from the charge reaction and how much from the gassing reaction. The following equation (6) indicates how the resistance R_i can be broken up into these two parts. To this end, equation (4) is used to obtain

$$I^2 R_i = (U-0.97U_o)\, I_{CR} + (U-U_{oE})I_{EC} \tag{5}$$

$$R_i = \underbrace{\frac{U-U_o}{I} \cdot \frac{I_{CR}}{I}}_{\text{Term 1}} + \underbrace{\frac{U-U_{oE}}{I} \cdot \frac{I_{EC}}{I}}_{\text{Term 2}} \tag{6}$$

Term 1 is the charge reaction dependent part and term 2 is the gassing reaction dependent part of the resistance. $(U-U_o)$ and $(U-U_{oE})$ in equation (6) are nonlinear functions of the charge current I. If the rate of charge of the battery and the charge current are low enough then the nonlinearity is not very strong as is seen in Fig 1 for the current voltage curves A, B, C, and D. So, for moderate charge currents, linear behavior of the current-voltage relationship of the battery can be assumed. Since gassing at the low state of charge is virtually absent, all current is used in the charge reaction. Thus $I_{CH}/I=1$ and $I_{EL}/I=0$ so that equation (6) reduces to

$$R_i = \frac{U-U_o}{I} \tag{7}$$

Since the gradient of the current-voltage relationship at the low state of charge is steep, R_i is small. It changes only marginally with increasing state of charge (see curves A, B, C in Figure 1). However, when the state of charge has increased sufficiently, then the resistance to the charged particle transport in the cell increases dramatically due to the depletion of $PbSO_4$ at the electrodes, as was discussed in Section 2. This is evident by a sharp

decline in the gradient of the current-voltage relationships (Curves D, E, F and G in Figure 1 turn into the horizontal direction) at sufficiently high currents. Thus, term 1 of equation (6) experiences a strong increase and this signals that the battery current approaches the limit of charge acceptance. It means that even arbitrarily large currents will not cause an increase of the current consumed in the charge reaction beyond a limit .

It can be seen from equation (6) and the curves in Figure 1 that R_i can easily grow to multiples of the value at the beginning of charge as the battery approaches the charge acceptance limit. It is therefore a suitable parameter for determining of how much current should be delivered by the charger.

It is emphasized here that R_i is not the gradient or derivative itself of the current-voltage curves in Figure 1 at a perticular cell voltage, although it depends on the gradient as the relationship (6) indicates. However due to the quasilinearity of the current-voltage relationship at low state of charge, the gradient of curves A,B,C is very closely the value of R_i.

As the state of charge increases, constant current charging results in an increase of R_i. Let us suppose a limit of R_i was defined and if R_i has reached this limit, a step-wise reduction of current is initiated. Then, limiting R_i that way limits the heat production in the cell even if the battery is not gassing. This is an advantage of R_i controlled charging over gas rate controlled charging using a gas rate sensor, which limits only the gas development i.e. reduces the charge current only if the battery gasses. High heat production in the battery reduces efficiency and battery life as well as does gassing.

While the state of charge increases and the current is reduced step-wise to limit R_j, the battery moves from curve D to E, F and G (Figure 1) and eventually reaches the gassing regime of voltage. As soon as gassing begins, it shares in the consumption of the current delivered by the charger and term 2 of equation (6) becomes non-zero, while $I_{CH}/I<1$. Because of the much larger overvoltage of the gassing reaction if compared to the charge reaction, the increase of term 2 is very strong, leading to a large increase of R_j as seen if Figure 6. The figure clearly indicates a close correlation between a strong increase of R_j and the onset of gassing. Even if the gassing current is only 15% of the charge current the gassing related part (term 2) of R_j can be as big as the charging related part (term 1) of R_j. As the percentage of the gassing current on the current delivered by the charger increases, R_j is increasingly determined by term 2. Because of the character of the current-voltage relationships for the gassing reaction and the charging reaction that were previously discussed, a reduction in the current when the battery is gassing is primarily a reduction in gassing current. It becomes increasingly so as the state of charge increases. Thus, limiting R_j during charging limits heat production at the low state of charge and gassing at the high state of charge. This completes the discussion of teh basic regulating mechanism used in the charge algorithm. It is thus clear that gas controlled charging could be done if R_j could be determined continuously during charging.

In the course of testing, it was found that the value of R_j could very closely be obtained by voltage and current measurements performed during pulse charging. This procedure calls for superimposing a current pulse on the base current and the measurement of the current increase ΔI and the voltage increase

ΔU due to the current pulsing. The ratio $R_j = \Delta U/\Delta I$ is an apparent resistance and numerically close to R_i as is seen in Figure 7. The reason why R_j equals so closely R_i is still speculation. A possible explanation is that because electrochemical reactions are slow, the additional current and voltage of the pulse reflect, during the short moment of pulsing, the losses of the charged particle transport through the battery before the pulsing, which means the response of the electrochemical reaction due to current pulsing is negligible if the pulse is sufficiently short. The current increase through the battey due to pulsing has only the supply of charged particles available that is provided by the electrochemical reactions before the pulsing. The corresponding voltage increases to facilitate the current should thus reflect the magnitude of energy losses that is experienced in the transport of the current through the cell and these losses are, as discussed previously, apparent as heat.

Based on the mechanism discussed in this section, the charge algorithm for charging the Hagen battery was designed. It is described in the next section.

3.4 Description of the Resistance Controlled Charge Algorithm

This section is a description of the charge algorithm now being used at the lighthouse test station of the U.S. Coast Guard Research and Development Center in Groton, CT. A flow chart of the control program is given in the Appendix 1 of this report. A copy of the HP BASIC program used in the HP controller in Groton is given in the Appendix 2.

The algorithm treats the value of R_j as an equivalent to the gassing rate and as a consequence of charge control produces a sequence of charge current steps. In its most fundamental form the algorithm requires the charge

controller at the beginning of charging to first determine the module that is most likely to start gassing first. The R_j value of this module is then obtained at the time when the module is not yet gassing i.e. at the beginning of charge. This R_j value is taken as a reference with which subsequent measurements of R_j that are made throughout the charging process, are compared. The R_j value of the module most likely to gas first is thus established as charge control feedback. If it exceeds a predefined multiple of the reference value R_{jref} then the charge current is stepped down which in turn reduces R_j with increasing state of charge, R_j increases again and the process of current reduction is repeated until an end-of-charge criterion is reached.

A charge algorithm must take into account a partially charged battery which tends to gas even at low charge currents. To make sure R_{jref} is measured when no gas is developed, charging starts at 4 A. At such a low current the battery needs some time to develop a significant gassing rate even if it is fully charged. Therefore, R_j if measured shortly after the charger is switched on to deliver 4 A, can be taken as reference value R_{jref}.

To establish R_{jref} the module voltages are measured in the control program 120 seconds after the start of the charge program and the module with the highest module voltage at 4 A is taken as a control module for which R_j values are determined. This is to prevent any of the modules from heavy gassing. Since gassing of the module requires that the module voltage exceeds the gassing voltage, the module with the highest voltage is most likely to reach the gassing stage first. By controlling its gassing development all other modules in the pack are also kept from gassing.

The reference value R_{jref} is now obtained by imposing a current pulse of approximately 10 A on the 4 A base current and by measuring the immediate voltage response of the control module to the current pulse. In practical terms: The voltage at 4 A charge current is measured, then the current is raised by about 10 A and within one second after the current raise the voltage is measured again. The ratio of the voltage increase to current increase is the reference value R_{jref}.

After the first current pulse, charging at 4 A constant current is continued for 2½ more minutes. This gives the battery sufficent time to develop significant quantities of gas if it is fully charged. Then the current is pulsed again to determine the R_j value and if the battery is in the gassing stage then this results in a R_j value that is substantially higher than the reference value. If gassing is severe enough to cause R_j larger two times R_{jref} then the charge current is reduced from 4 A by 0.3 A to 3.7 A, initiating the taper charge current phase from 4 A down to the end of charge as the current is decreased in steps of 0.3 A each time R_j exceeds the limit. If R_j is about equal to R_{jref} then the base current is raised to 10 A. Two and a half minutes after the increase of the charge current to 10 A, a 10 A pulse current is given on top of the 10 A base current to obtain the R_j value for a 10 A charge current Again the taper phase will be initiated if the R_j value is too high. Otherwise the charge current will be increased in steps of 5A each time checking the R_j value until 30 A is reached. At this point, a second and final value for R_{jref} is obtained. The charge controller will then hold this current constant until R_j is larger than two times the new R_{jref}.

This procedure is seen in the strip chart recording of Figure 8. It intends

to prevent any module from heavy gassing due to a high state of charge, low temperature or other conditions that cause poor charge acceptance. The algorithm is therefore independent of any condition causing low charge acceptance since charge acceptance is indirectly recorded through R_j throughout the charge process and the charge current is adjusted accordingly.

To account for the possibility that the module performance changes during charging, the module voltages are regularly compared at 30 A charge current at one minute intervals and R_j is determined for the module with the highest module voltage every 2½ minutes. The selection of the control module is thus updated. To obtain a tight control once the control module begins gassing, the pulsing interval for the determination of R_j is decreased from 2½ minutes to 10 seconds for the rest of the charge time. The strip chart recording of a typical charge is seen in Figure 9. The figure also indicates the gas development in the module with the highest module voltage. As seen, gassing is kept at low levels throughout charging.

Charging is terminated if the charge voltage of the control module exceeds 7.5 or if the charge current tapered to a value smaller than 2 A.

This completes the description of the charge algorithm. The implementation of the algorithm using U.S. Coast Guard hardware required some additional charge control features, since the program is based on current control while the diesel generator output is based on voltage control. The hardware and the necessary software interface to use the algorithm with the available hardware is discussed in the next section.

3.5 The Implementation of the Resistance Controlled Charge Algorithm in the Hybrid Power System.

For the implementation of resistance controlled charging in the hybrid power system, off-the-shelf hardware was used. This hardware is described in the next section. A schematic of the power system is seen in Figure 10.

3.5.1 Description of the Control Hardware.

Charge control is achieved by a Hewlett Packard HP 85 control computer that is interfaced via an IEEE 488 interface link with the HP 3852 S data acquisition and control system. All module voltages and a current signal from the battery shunt are input to the data acquisition system. Since multiplexed reed relays are used for the acquisition of module voltages these voltages are isolated as seen in Figure 11. Therefore the data acquisition system sees no voltage higher than 10 V which is an important advantage of the reed relay approach over a simple voltage divider to measure module voltages in a high voltage battery pack.

While the data collected as analog data from the battery are transmitted to the control system they are passing through an Amphenol 36-10P signal plug that is installed in the battery tray as seen in Figure 12. Table 1 associates each pin of the plug with a sensor on the battery. Each column in the Table 1 has a column number. Column (1) indicates the module number of the modules in the battery tray. These numbers are seen on labels attached to each module in the Hagen battery tray. Column (2) indicates the corresponding battery post to which a sensor was attached. Column (3) identifies the plug pin in the Amphenol connector that is attached to the tray. The identification symbol is engraved

beside each pin of the plug. Column (4) identifies the fuses on the fuse board. The fuse system is to protect the data acquisition system from damage in case of battery sensor malfunction. The fuse board is seen in Figure 13. The fuse numbers are placed on labels besides each fuse. Column (5) indentifies the card slot in the data acquisition system. The card slot number is obtained from the HP manual of the system. As seen, two slots are occupied. Each card in the slot carries 20 data acquisition channels labeled from 01 through 19. The channels are identified in column (6). Hence, Table 1 indicates that the positive post of module 6 is connected to pin C in the plug. Pin C connects to fuse number 102 and then to channel 18 in the first relay card.

The connections for a relay card section are again indicated in the wiring diagram (Figure 11) of a typical section of a relay card. On the figure it is seen that additional fuses are installed between the relays on the relay card. These connections are also indicated in column (7) of Table 1.

Since the Basler control board of the diesel generator accepts only a signal of approximatly 0-1V, the output voltage from the control system (0-10V) is translated to a 0-1V signal to increase resolution and achieve better control. The voltage output from the control system is proportional to a finite discrete number set sent by the control computer to the D/A board. If the set consists of 100 values corresponding to 0-10V then the range of 0-1V has only 10 steps (numbers) for control. The voltage divider, however, reinstalls all 100 steps of the 0-10V range to the 0-1V range. The schematic of the voltage divider is seen in Figure 14 (a). The power supply needed to drive the circut seen in Figure 14 (a) is seen in Figure 14 (b). Table 2 indicates the voltage transformation. The circuit is installed on the fuse board seen in Figure 13. This completes the discription of the hardware for the control system.

As discussed in the previous section, the charge algorithm uses current control for charge control. The diesel generator control board, however, controls output voltage. Therefore a control program had to be designed that controls diesel generator output voltage such as to maintain a constant current between current changes that are initiated by the charge control algorithm. A separate control program for current control was written and interfaced with the charge control program. The current control program is described in the next section.

3.5.2 Description of the Control of Current from the Diesel Generator.

Alternating current is produced by the diesel-powered alternator, which turns at a constant 1800 rpm. This AC current is rectified to DC to charge the battery. The magnitude of the AC current output is controlled by varying the current through the alternator field windings.

A feedback loop is used to govern the field current as follows: The computer (in this sense, the computer/data acquisition system) reads the DC current supplied to the battery from the shunt. If the current is too low, the computer outputs a decreased analog voltage. This voltage runs through the signal conditioner, which reduces it by a factor of 10. The reduced voltage proceeds to the Basler generator controller, which increases the alternator field current proportional to the decreased signal voltage. The increased field current increases the AC output and thereby the DC charge current from the rectifier. The computer reads the new current, and if need be sends the next analog output voltage to control the current again. Note that increasing the control voltage reduces the charge current and vice versa. Since the charge current can drift

rapidly for a given constant control voltage, especially in the early part of the charge, the computer spends most of its time in the current control loop. This loop is interrupted at various intervals, the frequencies of which depend on the state of change and the length of which do not exceed approximately two seconds. These interruptions are necessary for current pulsing, resistance calculation and scanning of battery parameters.

A current reading which is outside the desired current by more than 0.1 A results in a change to the control output. The desired current is a product of the resistance controlled charge algorithm.

3.6 The Effect of the Charge Algorithm on the Battery under Special Operating Conditions.

This section is an attempt to qualify the battery response to the charge algorithm under out-of-the-ordinary operating conditions. It is only an attempt, because a systematic test program in this respect was not conducted. The value of such an analysis is primarily for crisis control. Since the hybrid power system is a self-sufficient independent power system with extremely long maintenance intervals it should have at least limited "self-healing" capabilities that will prevent the system from a complete breakdown in the event of a partial failure. To this end an on-board analysis system is needed to evaluate the performance of components of the system, in particular of the battery which is one of its most sensitive components, and to initiate a reorganization of the charge and load schedule.

Such self-healing capabilities could be in terms of changes in the charging schedule due to a malfunctioning battery cell or terminal connector, induction

of equalization charges after a long period of partial discharges, automatic shunting of shorted battery cells, redistribution of the operational load between battery and diesel by redefining the end-of-discharge voltage when either the diesel indicates problems by losing power or the battery is near the end of life. These functions are by no means a complete set, but serve only as illustrations here. A complete identification of measures that could be undertaken to improve the reliability of the system should clearly be one of the objectives of future work. As far as the battery is concerned, those measures should be based on the status and performance of the battery which are indicated by voltage and current measurements and by the time it takes to charge the battery.

The algorithm is designed to charge correctly with a high degree of independence from the status of the battery. It takes automaticaliy into account the most likely changes in battery performance due to changes in temperature, state of charge and battery age. This is done by continuously comparing the battery module voltages during charging among each other and with those at the beginning of charge. Invariably the battery responds to any kind of problem with current reductions to enforce moderate module voltages and voltage differences. Therefore a battery problem will show up as unusually long charge and short discharge. The general response is to treat a problem battery as a battery with reduced capacity and charge it as gently as possible.

This way some battery problems can be "healed". An unbalanced battery pack will in the course of serveral cycles be equalized. A battery with a bad battery connector will in the course of several cycles be current limited, thus avoiding a battery post melt-down. A battery with frozen electrolyte will be gently heated up thus avoiding the boiling out the electrolyte.

In a more sophisticated analysis, battery problems will show up as low battery efficiency and a gradual steady decline in capacity. With proper communication links the controller could alarm a distant operator that maintenance might be needed.

This type of analysis and control of the system has been dealt with only on a very fundamental level in the present project. But more work, specifically on defining specific criterions that allow to identify battery problems from battery behavior and indicate a need for response in the organization of the system operation, is clearly needed. Technology of this kind is quite generally in its infancy, with the first companies trying to specialize in "battery control." So, the need of such technology has been generally acknowledged, but actual systematic work on which the hybrid system for lighthouses with its especially stringent reliability requirements could build on, has not been done.

4.0 SUMMARY

Proper charging was identified as the most important requirement for the reliable and economical operation of a battery that is part of the hybrid power system for remote lighthouses. Therefore a charge algorithm was developed to optimize charging of a flooded lead-acid battery with forced electrolyte destratification. This algorithm is independent of the operating temperature, the state of charge and the battery age. It controls charging according to the weakest battery module in the pack and is able in the course of several cycles to automatically equilize the performance of the modules in the battery pack without excessive overcharging. The charge algorithm prevents overheating due to bad battery connectors and quite generally responds to all causes of poor charge acceptance with a gentle treatment of the battery during charging.

The charge algorithm is a follow-up development of the UAH charge algorithm that was previously developed at the EEPL for the U.S. Department of Energy. But in contrast to the UAH algorithm the new algorithm does not need a gas rate sensor and is able to account for the weakest module in the pack. As is the case with the UAH algorithm, the new algorithm limits gassing, but it also limits excessive heat production from other sources than gassing. It is therefore particularly suited for remote applications where no operator is available to take corrective action.

The new algorithm monitors during charging all module voltages and the current of a high voltage battery and uses current pulsing to determine the electric battery resistance that is responsible for the heat development in the battery. The charge current is controlled by limiting the resistance of the weakest module in the pack.

To justify the validity of this concept, it was shown that the heat development in the battery can be expressed in terms of the overvoltages of the charge reaction and the gassing reaction; further that the heat development is mainly a consequence of losses caused by the transport of charged particles from one electrode to the other which can be interpreted in terms of an apparent electrical resistance. This resistance was shown to be very closely the ratio of WU/WI during pulsing. It was formally divided into two parts, one associated with the charge reaction, the other one associated with the gassing reaction and by doing so, it was shown that limiting the resistance through current control causes the heat development in the battery to be limited at low state of charge and gas development to be limited at higher state of charge. It works because of the difference in the nonlinear current-voltage relationships of the gassing reaction and the charging reaction and because of the large differences in overvoltage needed for these two reactions to occur. Charge tests were conducted to verify the validity of the charge algorithm.

List of References

[1] D. Nowak "A State of Charge and Temperature Independent Charge Algorithm for Flooded Lead-Acid Battery Packs." Final report prepared for The Aerospace Corporation under contract No. W-0384 NV, 1985

[2] D. Nowak, "The Effect of Current Pulsing on Electrolyte Destratification" Final Report for the Dep. of Energy, in preperation.

Table 2

In-and Output Voltage of the Signal Conditioner for the Diesel Control Voltage (See Fig 14)

IN	OUT
10	.99
9	.891
8	.792
7	.693
6	.593
5	.494
4	.395
3	.296
2	.197
1	.097
.9	.087
.8	.077
.7	.068
.6	.058
.5	.048
.4	.038
.3	.028
.2	.018
.1	.008
.05	.003
.025	.001
0	-.001

Table 1

Connections Between Battery and Data Acquisition System

HAGEN MODULE NO (1)	BATTERY POST (2)	PLUG PIN (3)	FUSE NO (4)	D/A CARD NO (5)	CHANNEL NO (6)	RELAY CONNECTION (7)
6	+	C	102	1	18	
12	+	D	103	1	12	
20	+	E	104	1	04	
19	+	F	105	1	05	
18	+	G	106	1	06	
17	+	H	107	1	07	
16	+	I	108	1	08	
15	+	J	109	1	09	
14	+	K	110	1	10	
13	+	L	111	1	11	
13	-	M	112	1	12	
11	+	N	113	1	13	
10	+	P	114	1	14	
9	+	Q	115	1	15	
8	+	R	116	1	16	
7	+	S	117	1	17	
6	-	T	118	1	18	
5	+	U	119	1	19	
4	+	V	200	2	00	
3	+	W	201	2	01	
3	-	X	202	2	02	
2	+	Y	203	2	03	
1	+	Z	204	2	04	
1	-	a	205	2	05	

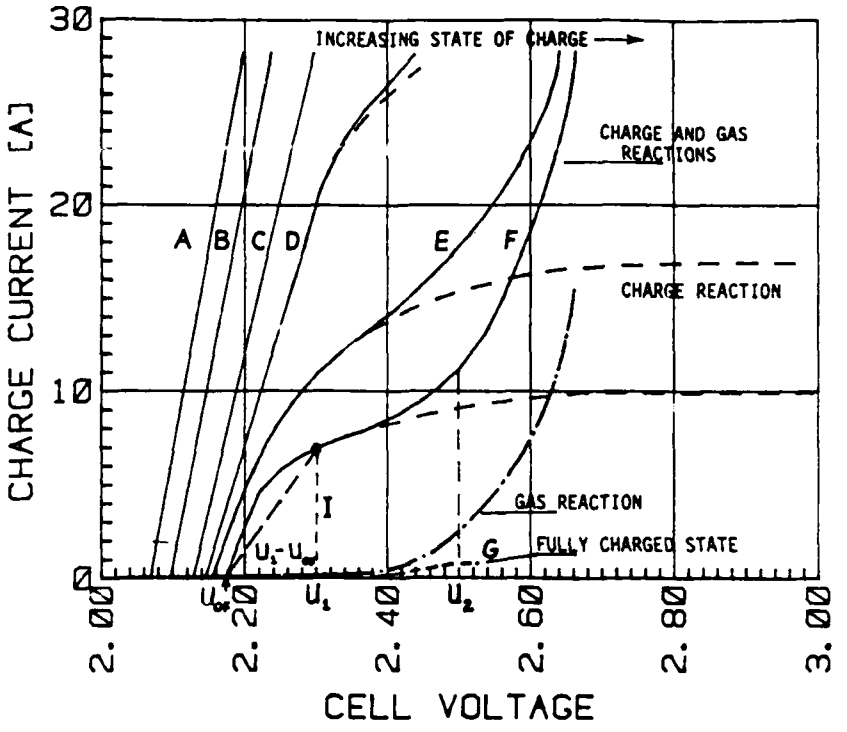

Figure 1. Current-Voltage Relationships for the Charging Process of a Lead-Acid Battery at Various State of Charge

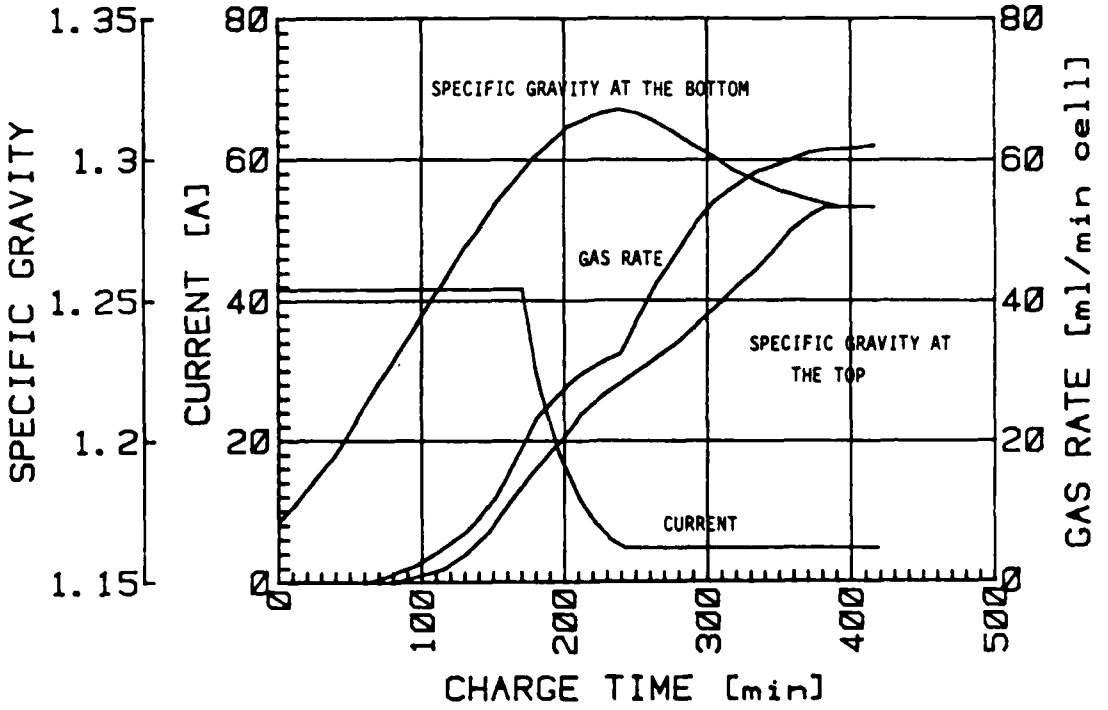

Figure 2. Development of the Specific Gravity at the Bottom and Top of a Lead-Acid Cell During a Conventional Charge

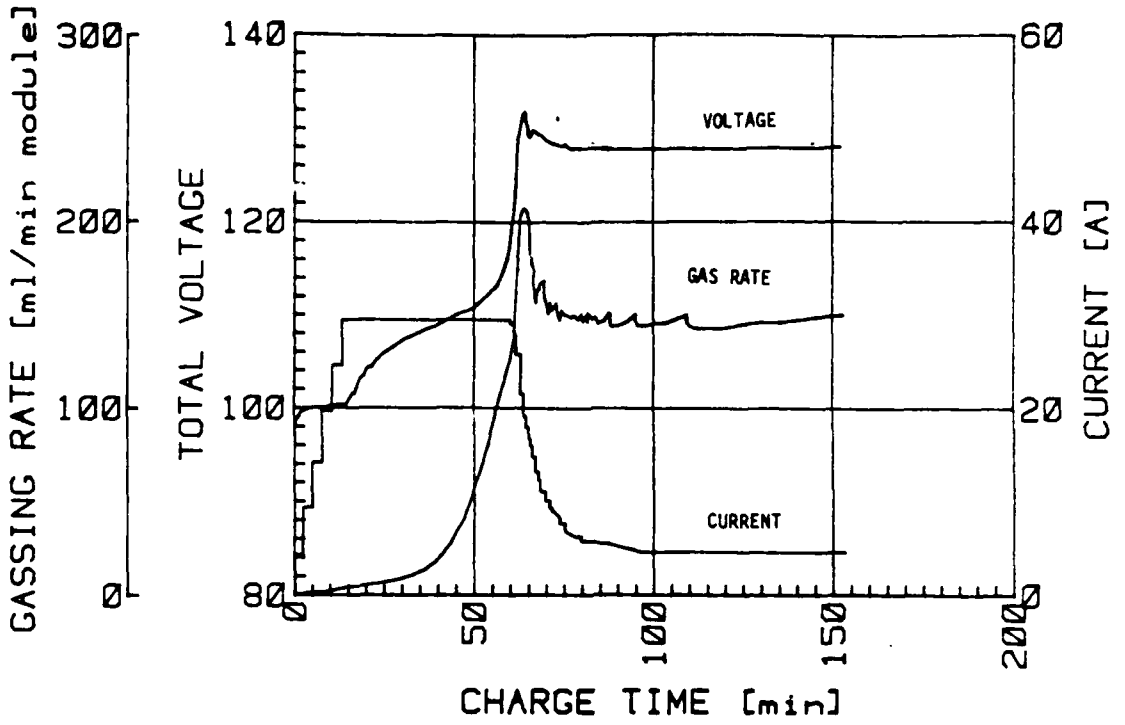

Figure 3. Voltage, Current and Gas Development During Charging with the UAH Algorithm

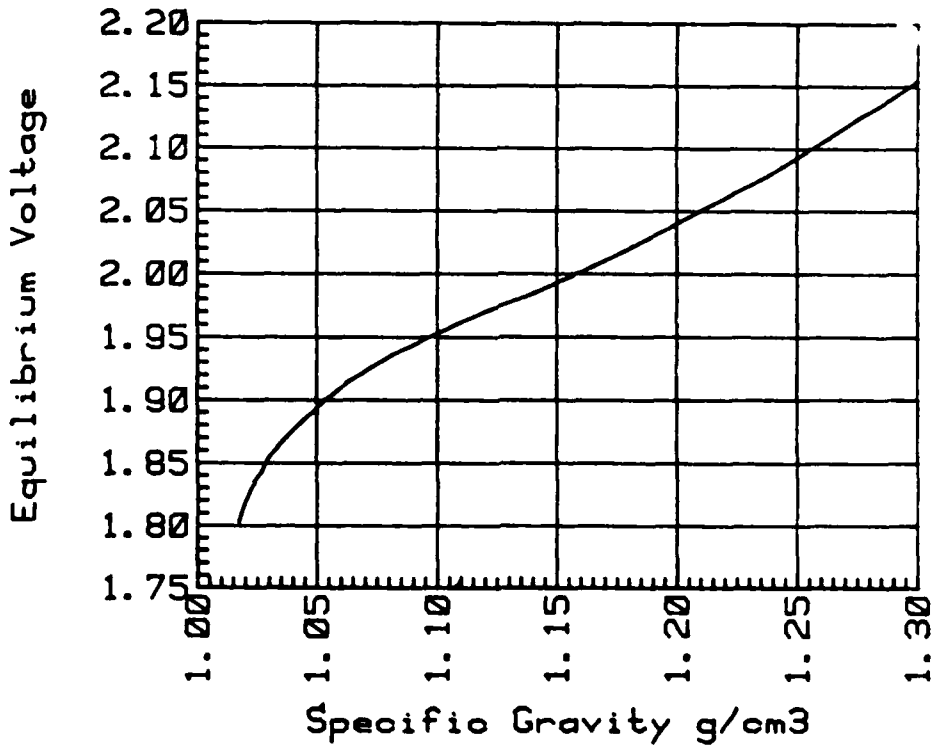

Figure 4. Electrolyte Density as a Function of Equilibrium Voltage

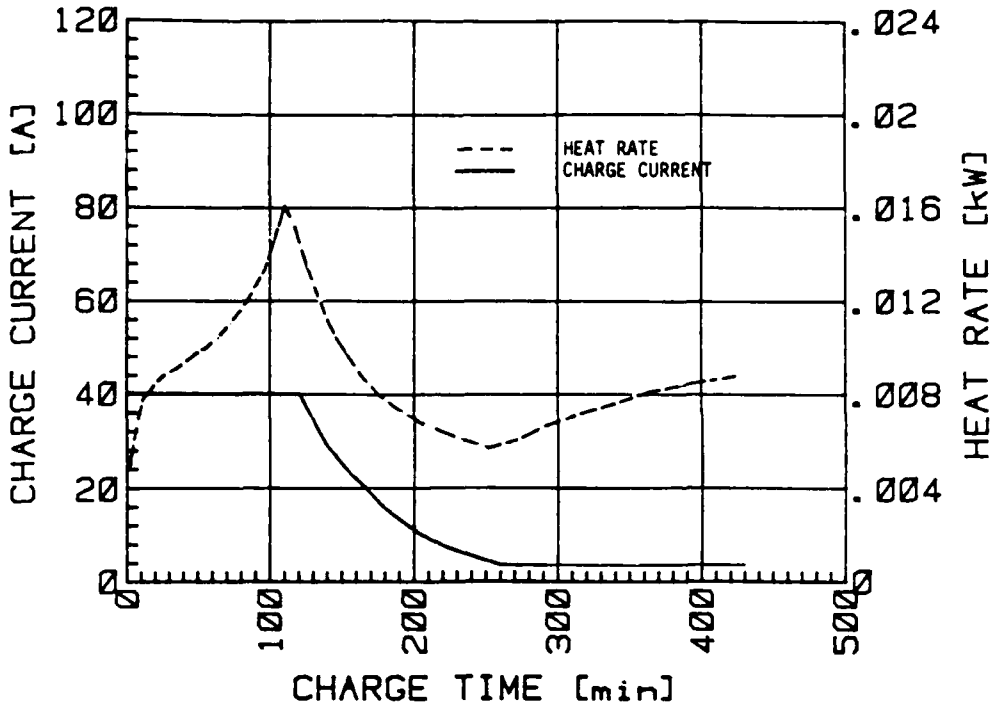

Figure 5. Heat development During Conventional Charging

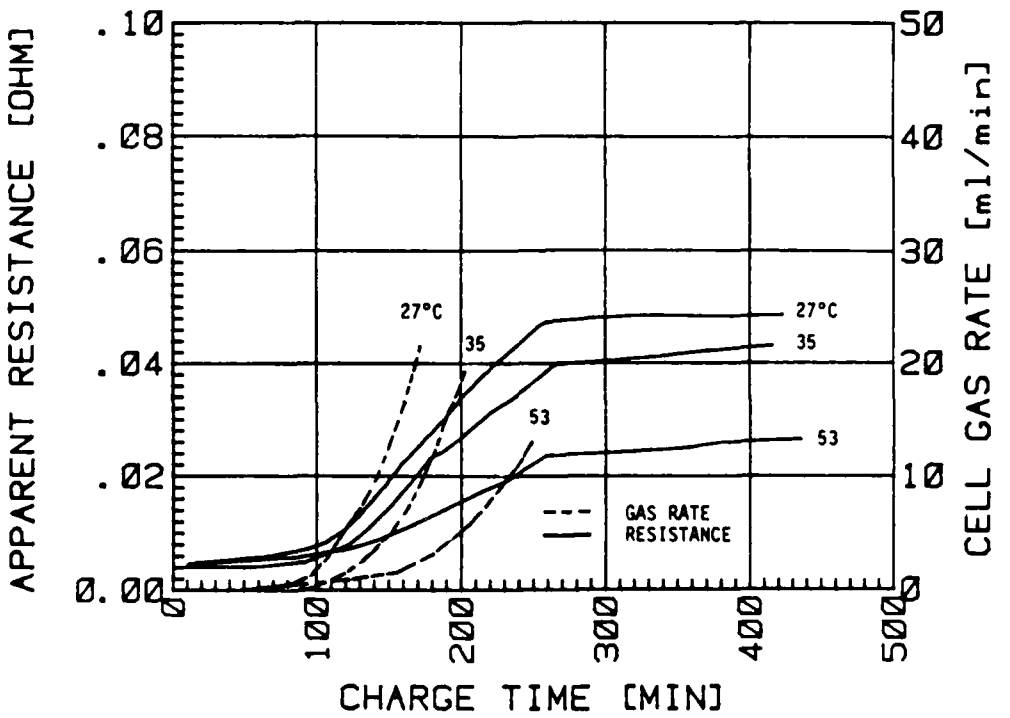

Figure 6. The Development of the Electric Resistance that is Responsible for Battery Heat-up and Development of the Gas Rate During Conventional Charging at Various Operating Temperatures

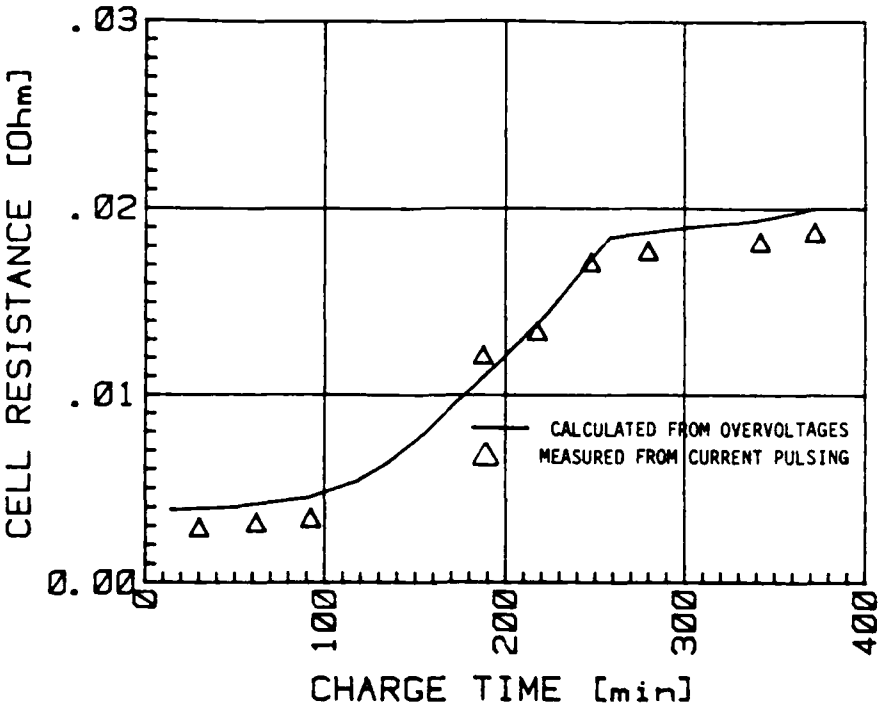

Figure 7. The Apparent Cell Resistance Development During Charging Calculated from Overvoltages (see also Figure 6) and Measured from Current Pulsing: $R_i = \Delta U/\Delta I$

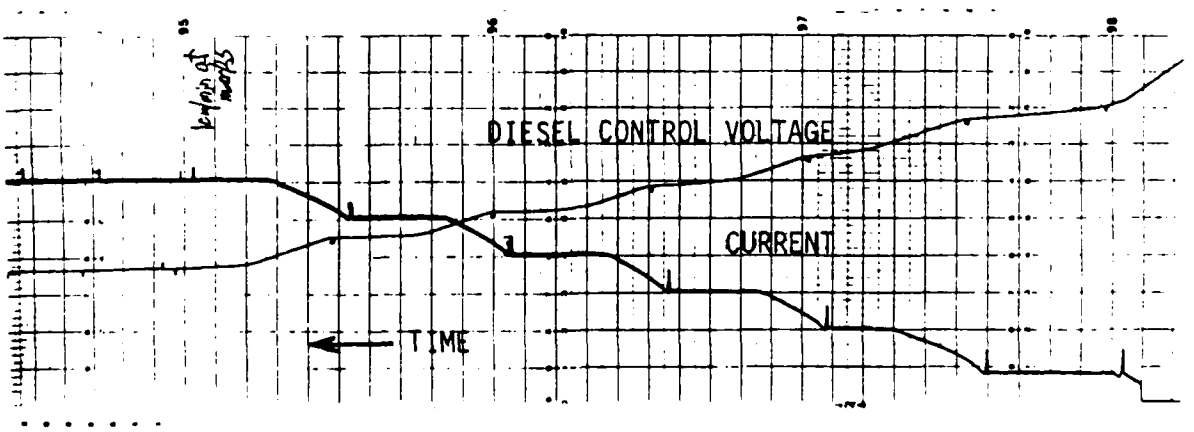

Figure 8. Initial Current Ramp and the Corresponding Control Voltage for the Diesel Generator During Pulse Charging

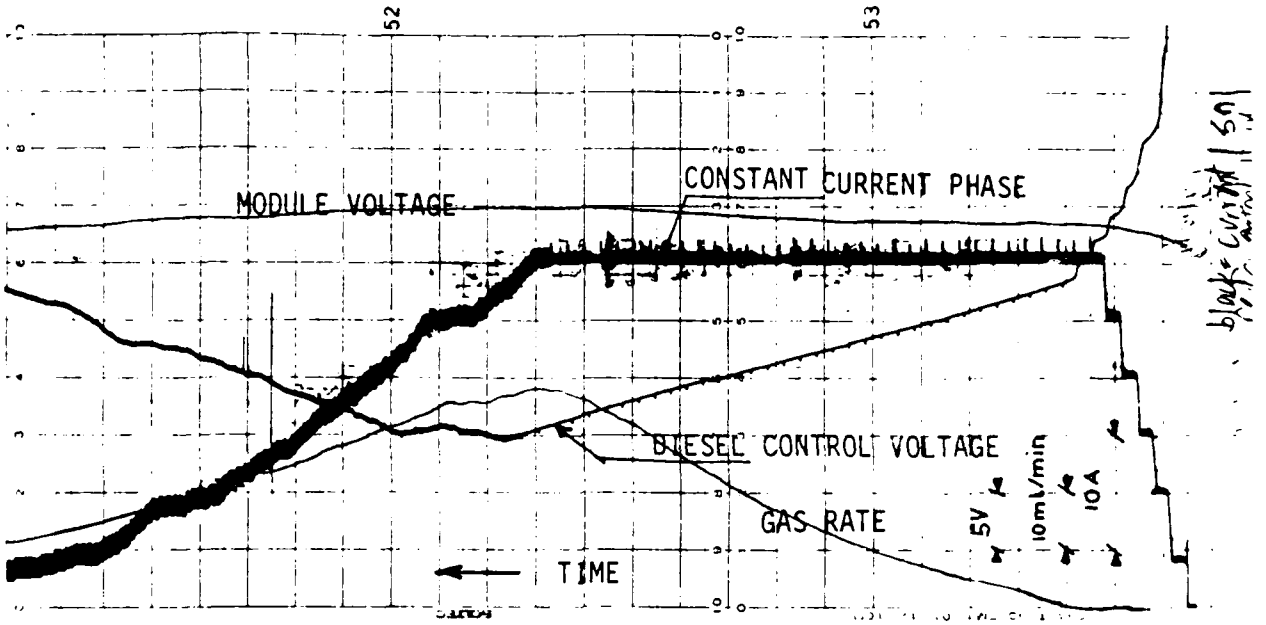

Figure 9. Strip Chart Recording of Charge Current, Control Voltage for Diesel Generator and Gassing Rate During Pulse Charging

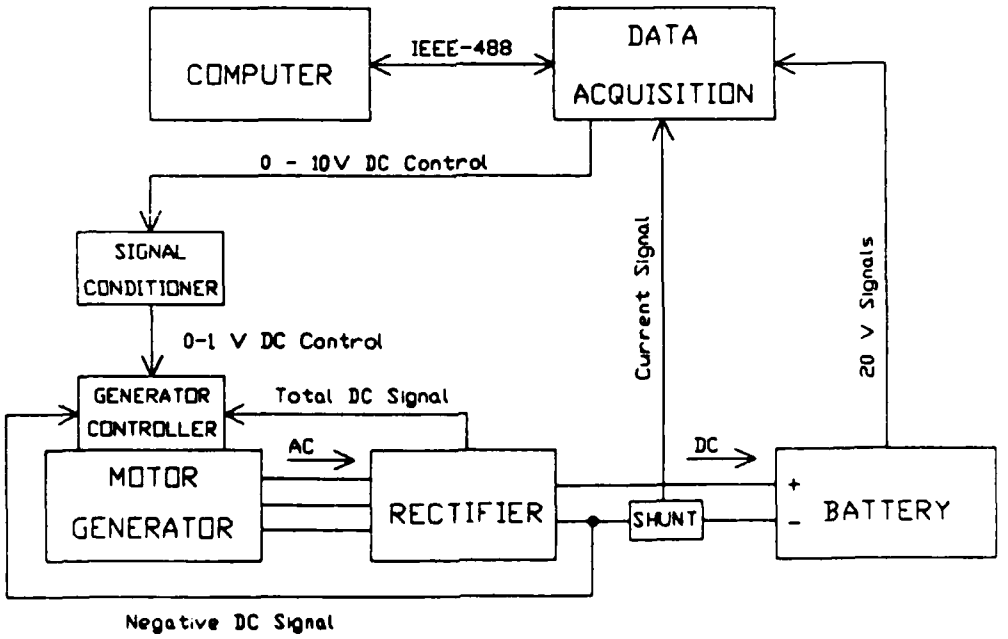

Figure 10. Schematic of the Hybrid Power System

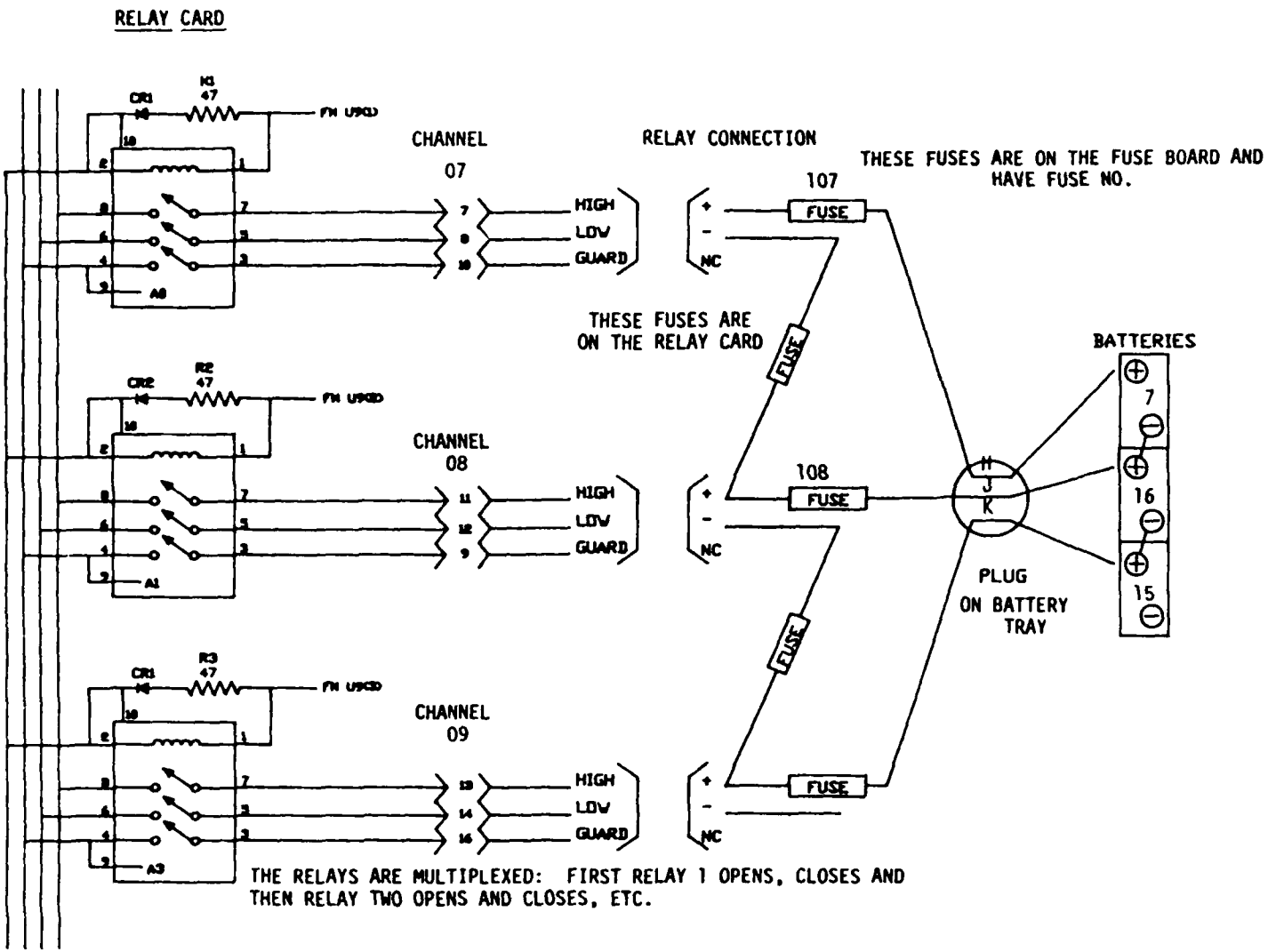

Figure 11. Schematic Section of the Wiring Diagram of the Battery and Charge Controller

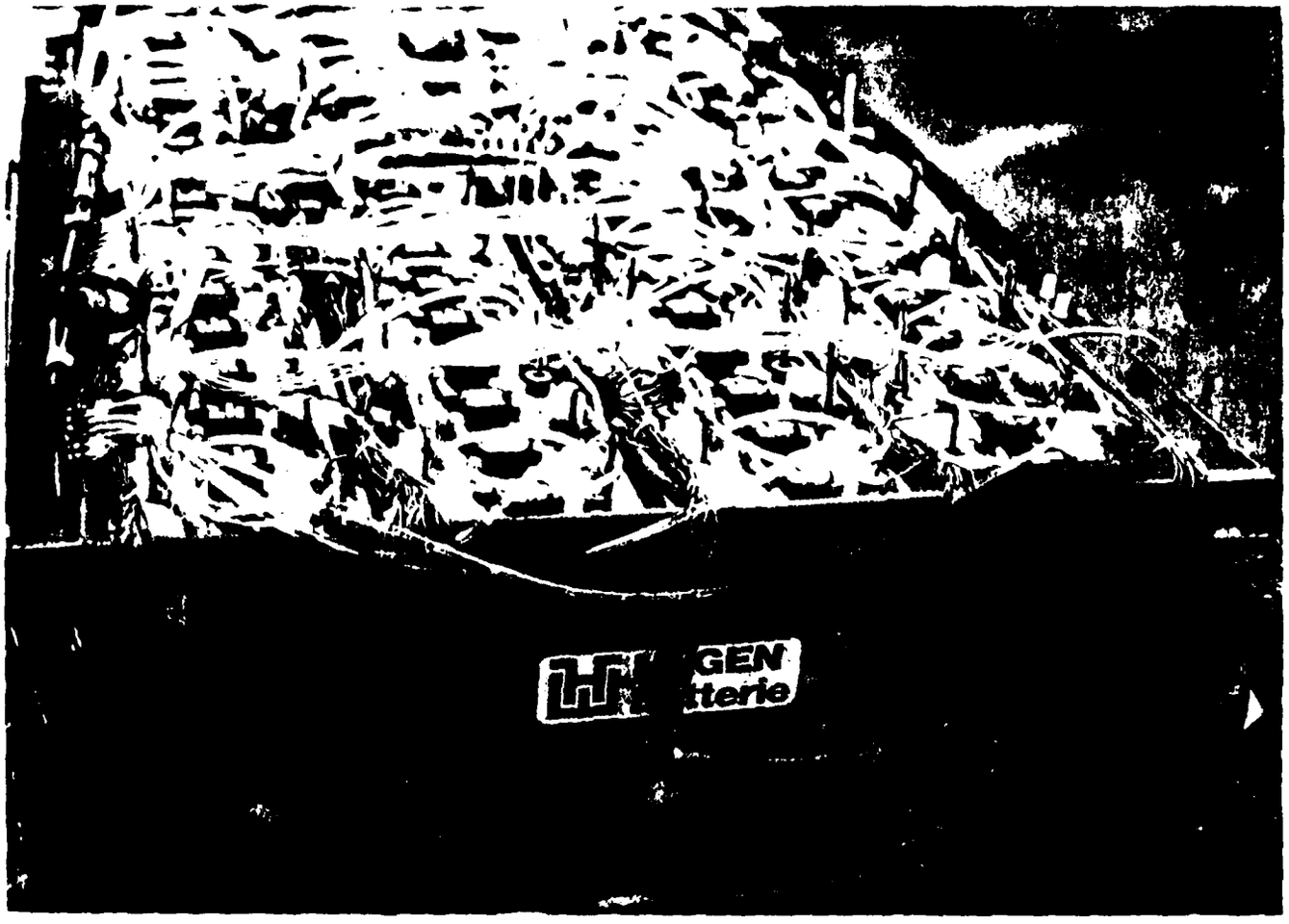

Figure 12. Hagen Battery Tray

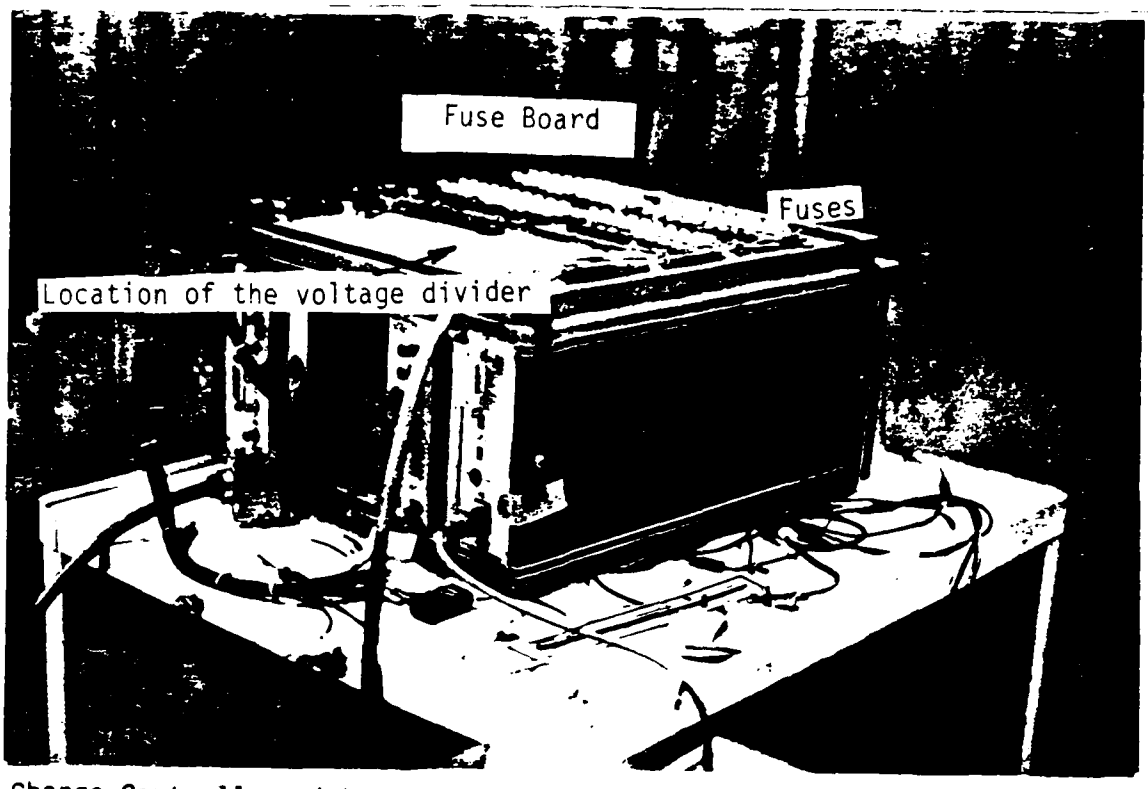

Charge Controller with Fuse Board

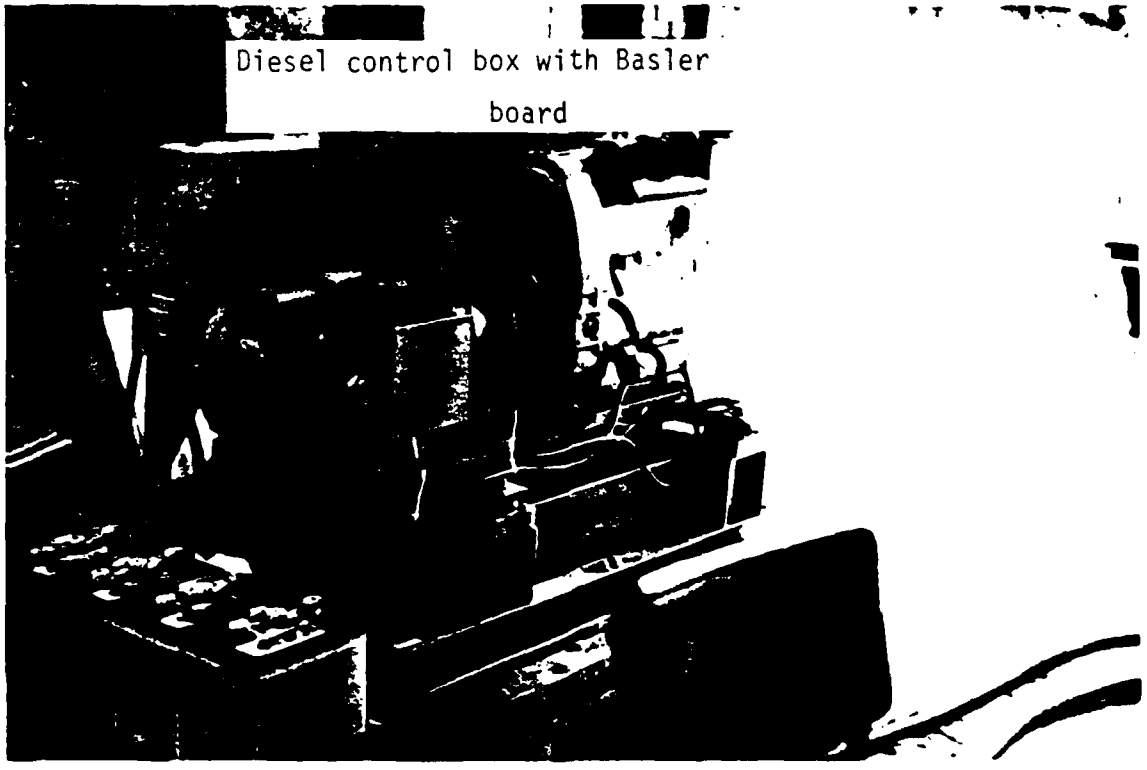

Figure 13. Charge Controller and Lister Diesel Generator

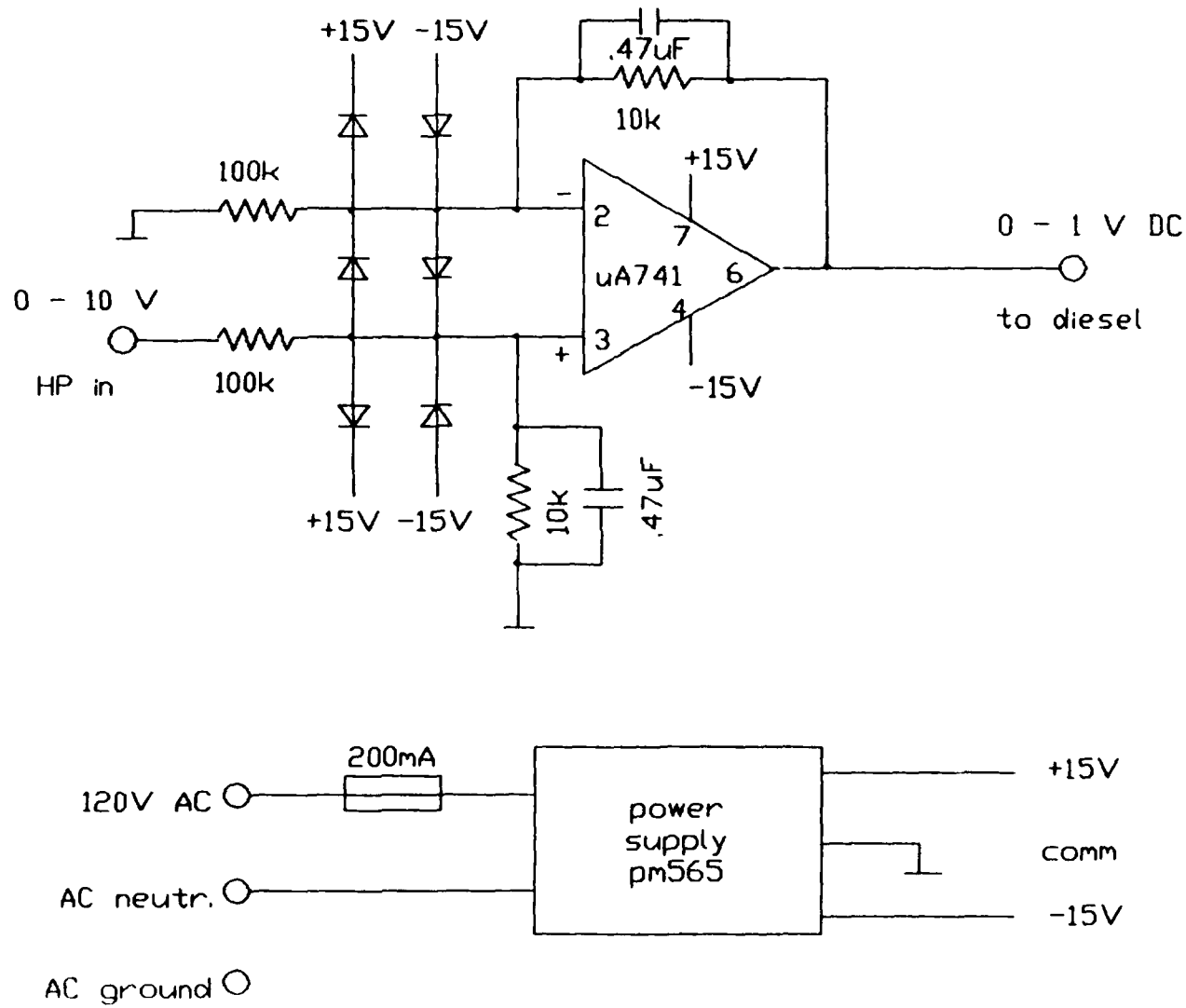

Figure 14. Signal Conditioner for Diesel Control Voltage

APPENDIX 1

FLOW CHART OF THE RESISTANCE CONTROLLED CHARGE ALGORITHM

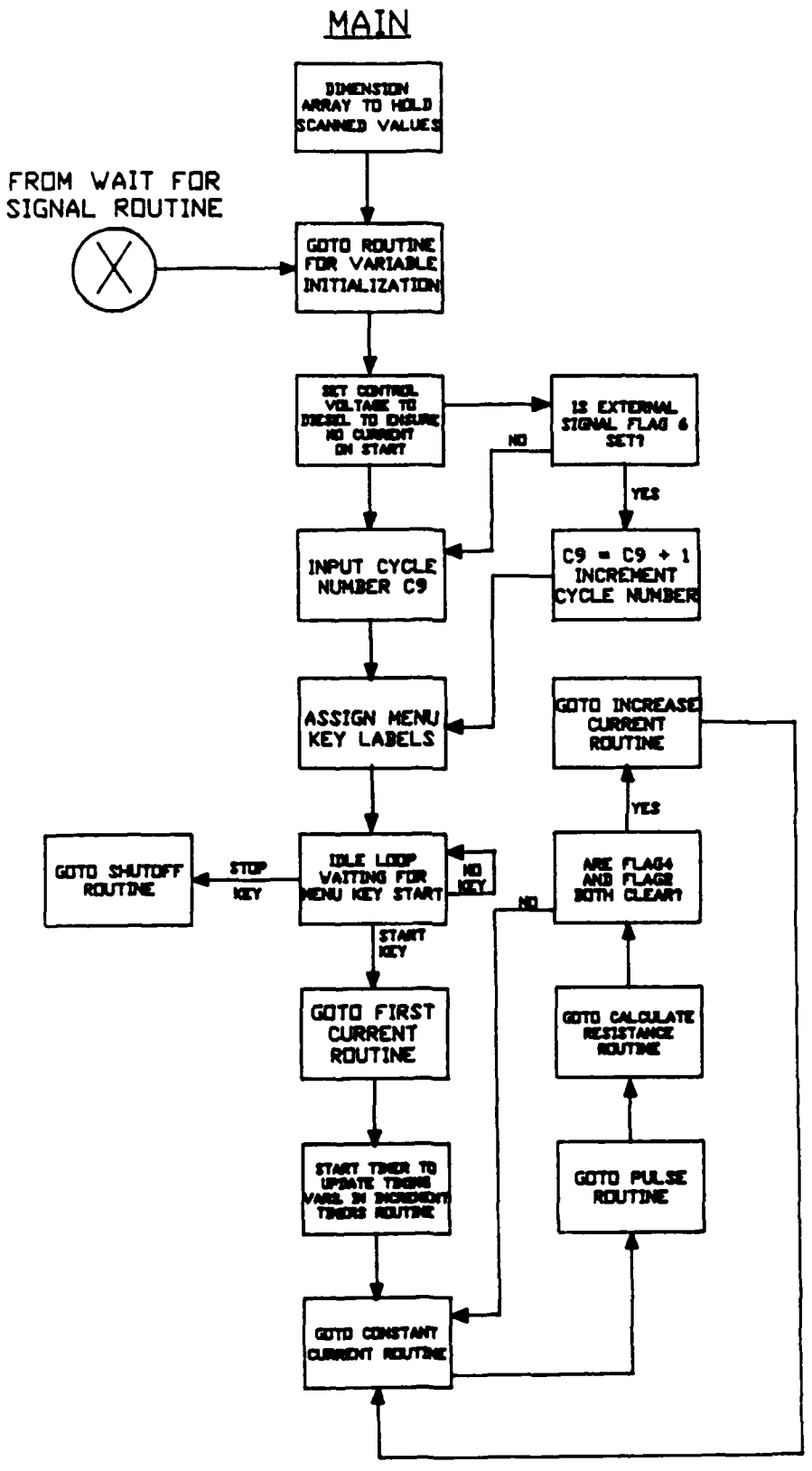
MAIN
DIMENSION ARRAY TO HOLD SCANNED VALUES
FROM WAIT FOR SIGNAL ROUTINE
GOTO ROUTINE FOR VARIABLE INITIALIZATION
SET CONTROL VOLTAGE TO DIESEL TO ENSURE NO CURRENT ON START
IS EXTERNAL SIGNAL FLAG 6 SET?
NO
YES
INPUT CYCLE NUMBER C9
C9 = C9 + 1 INCREMENT CYCLE NUMBER
ASSIGN MENU KEY LABELS
GOTO INCREASE CURRENT ROUTINE
YES
GOTO SHUTOFF ROUTINE
STOP KEY
IDLE LOOP WAITING FOR MENU KEY START
NO KEY
ARE FLAG4 AND FLAG5 BOTH CLEAR?
NO
START KEY
GOTO FIRST CURRENT ROUTINE
GOTO CALCULATE RESISTANCE ROUTINE
START TIMER TO UPDATE TIMING VARS IN INCREMENT TIMERS ROUTINE
GOTO PULSE ROUTINE
GOTO CONSTANT CURRENT ROUTINE

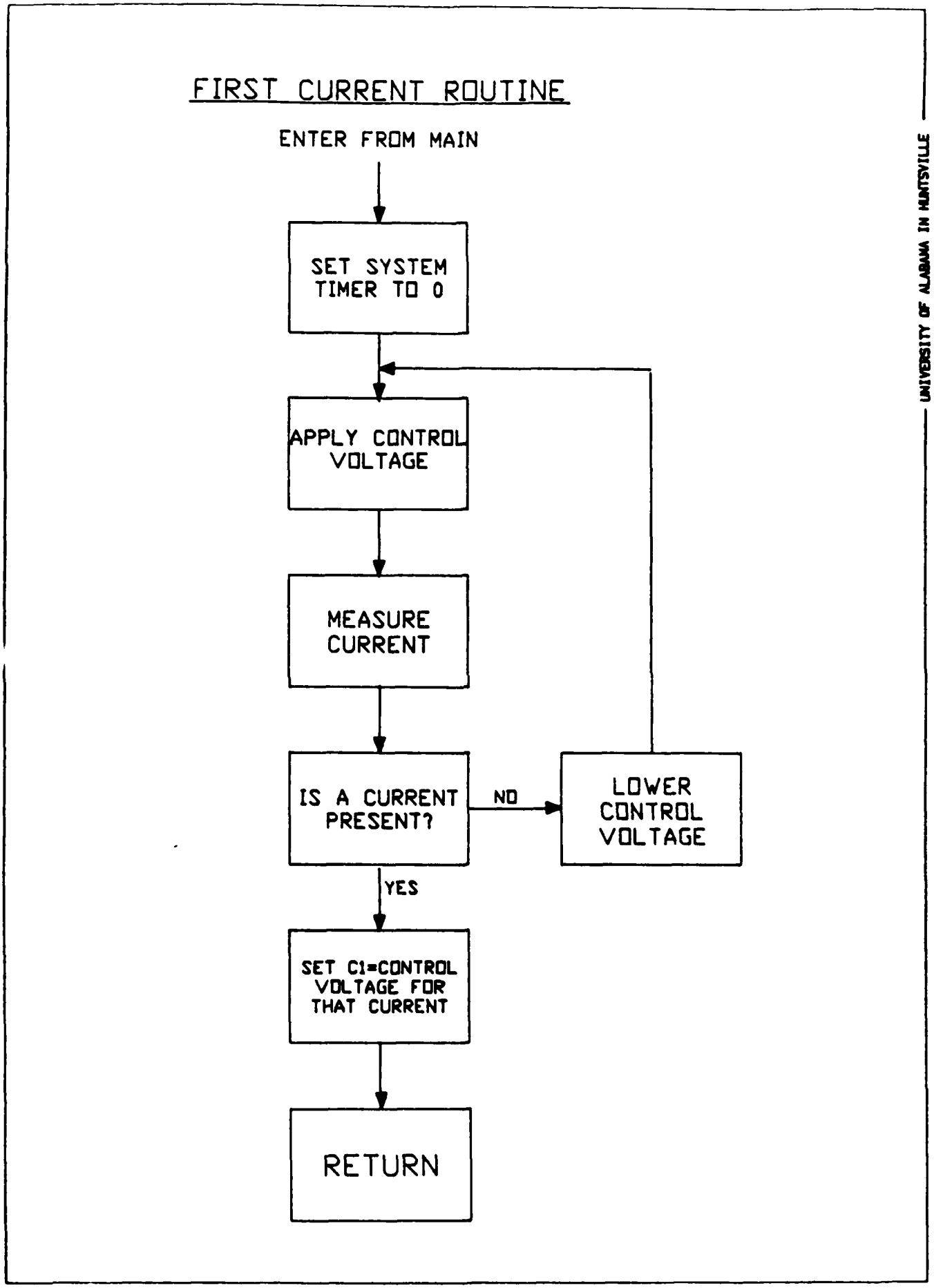

SHUTOFF SUBROUTINE

ENTER FROM: MENU KEY IN MAIN
APPLY PULSE ROUTINE
LOWER CURRENT ROUTINE

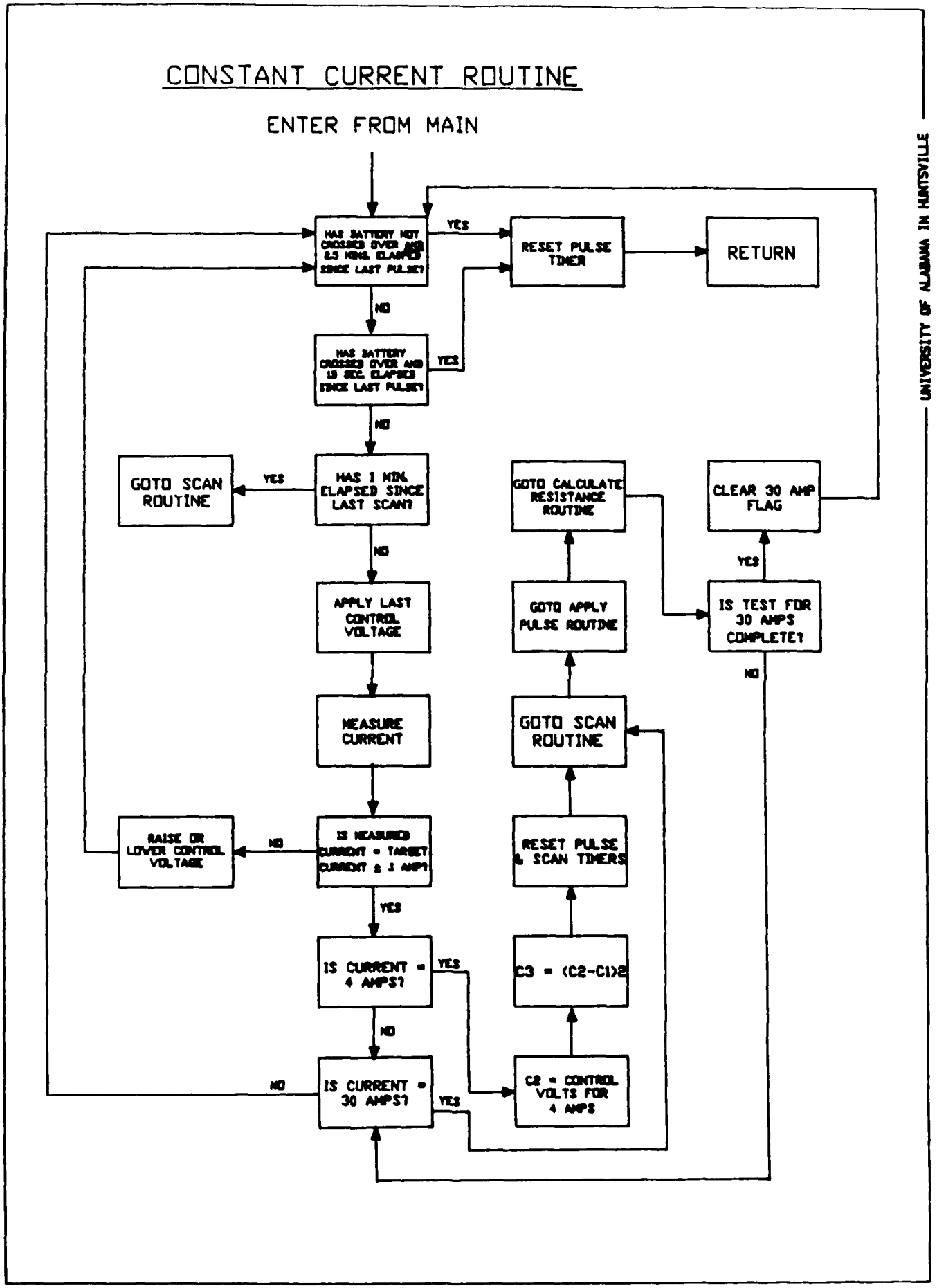
CONSTANT CURRENT ROUTINE
ENTER FROM MAIN
HAS BATTERY NOT CROSSED OVER AND 0.5 MIN. ELAPSED SINCE LAST PULSE?
YES
RESET PULSE TIMER
RETURN
NO
HAS BATTERY CROSSED OVER AND 15 SEC. ELAPSED SINCE LAST PULSE?
YES
NO
GOTO SCAN ROUTINE
YES
HAS 1 MIN. ELAPSED SINCE LAST SCAN?
GOTO CALCULATE RESISTANCE ROUTINE
CLEAR 30 AMP FLAG
NO
APPLY LAST CONTROL VOLTAGE
GOTO APPLY PULSE ROUTINE
YES
IS TEST FOR 30 AMPS COMPLETE?
MEASURE CURRENT
GOTO SCAN ROUTINE
NO
RAISE OR LOWER CONTROL VOLTAGE
NO
IS MEASURED CURRENT = TARGET CURRENT ± .1 AMP?
RESET PULSE & SCAN TIMERS
YES
IS CURRENT = 4 AMPS?
YES
C3 = (C2-C1)2
NO
NO
IS CURRENT = 30 AMPS?
C2 = CONTROL VOLTS FOR 4 AMPS
YES
UNIVERSITY OF ALABAMA IN HUNTSVILLE

APPLY PULSE ROUTINE

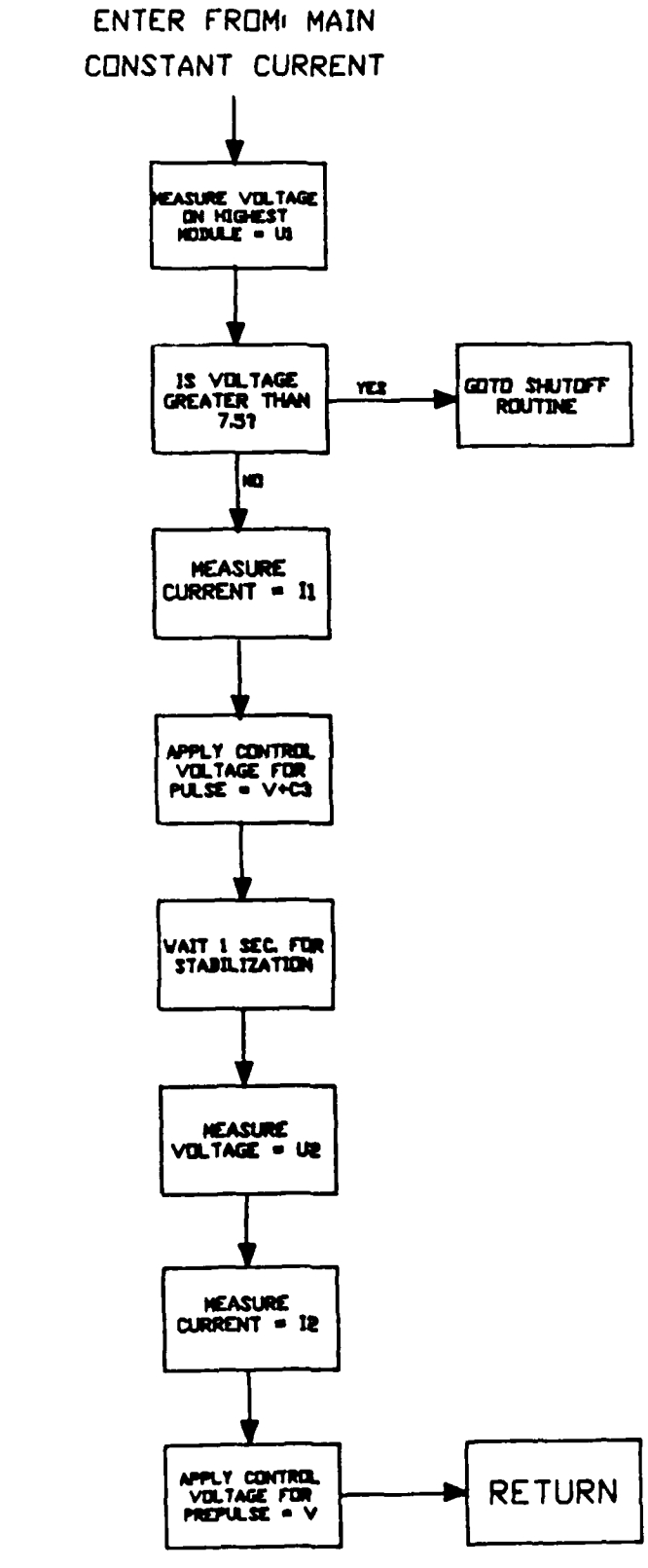

CALCULATE RESISTANCE ROUTINE

ENTER FROM: MAIN CONSTANT CURRENT ROUTINE

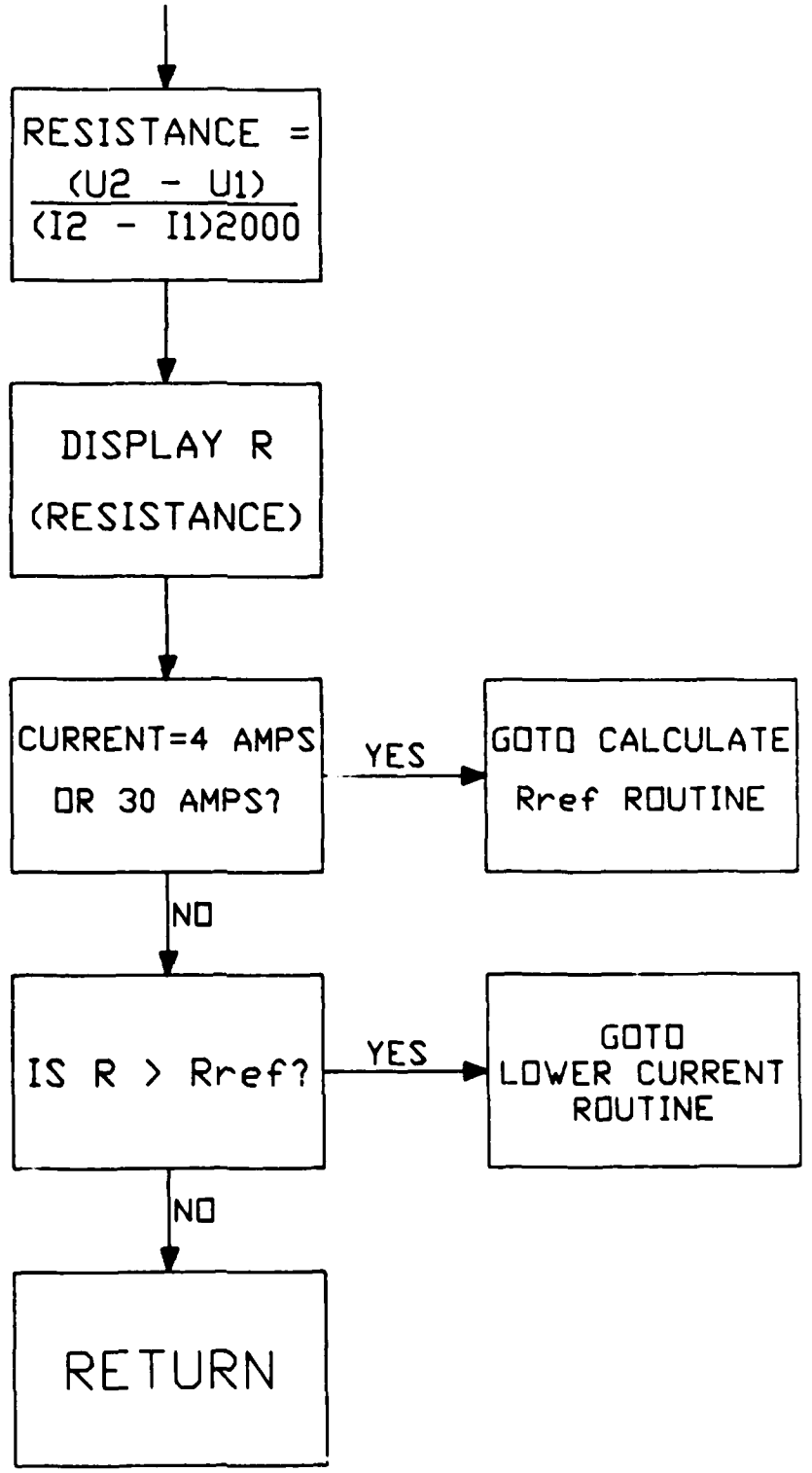

INCREASE CURRENT ROUTINE

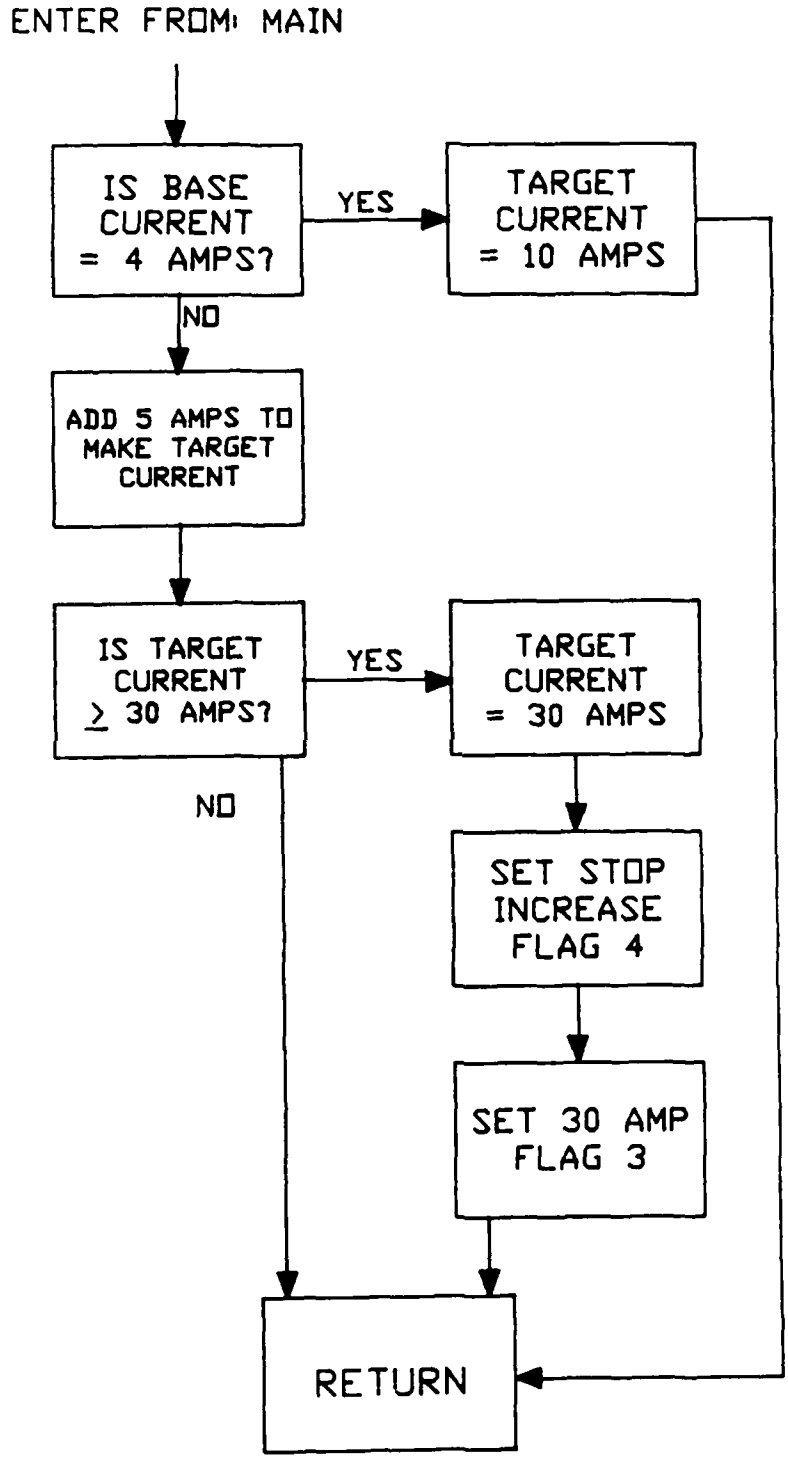

LOWER CURRENT ROUTINE

ENTER FROM:
CALCULATE RESISTANCE ROUTINE

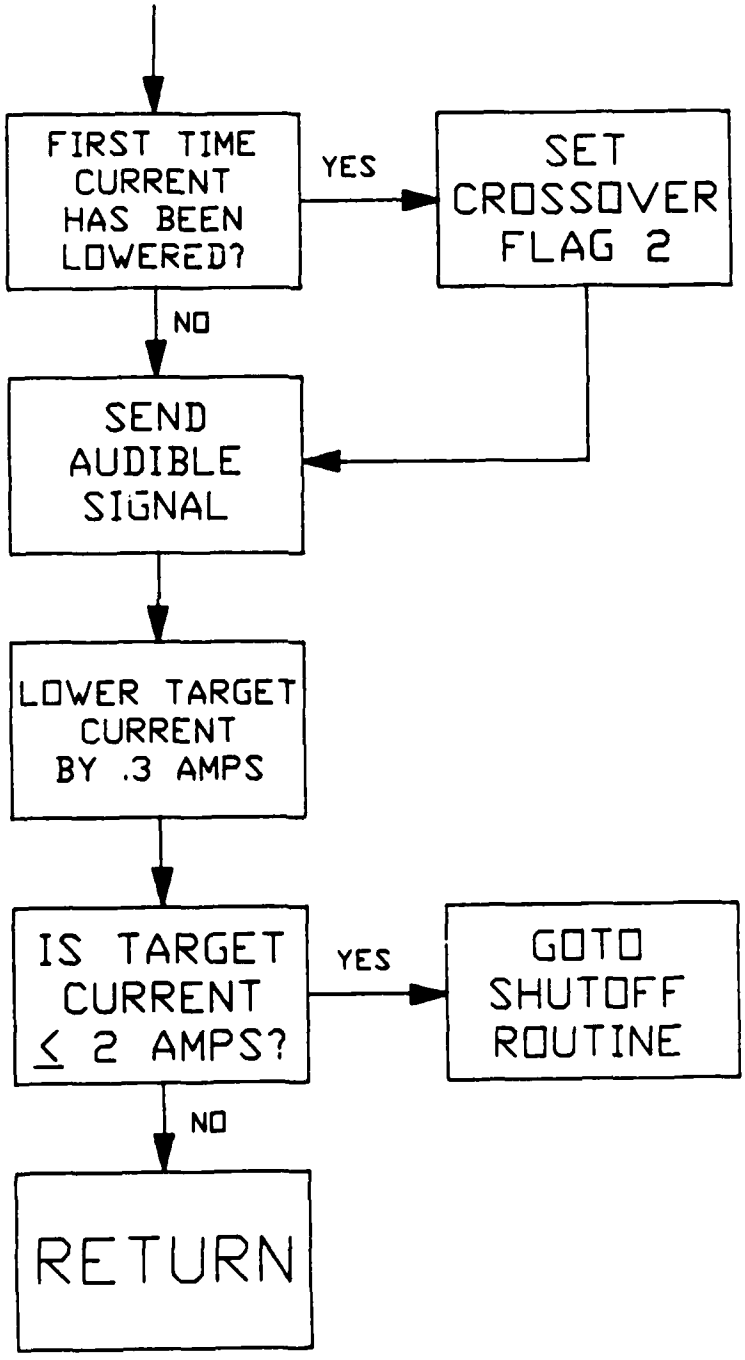

CALCULATE Rref ROUTINE

ENTER FROM CALCULATE RESISTANCE ROUTINE

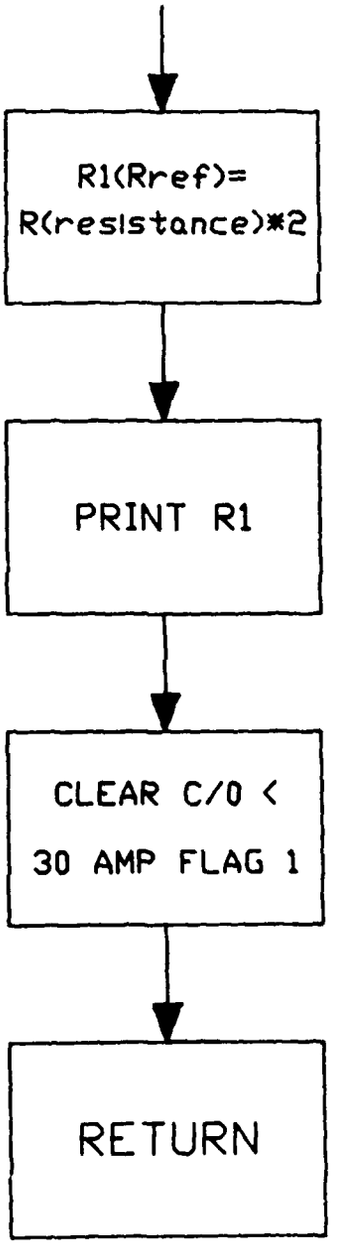

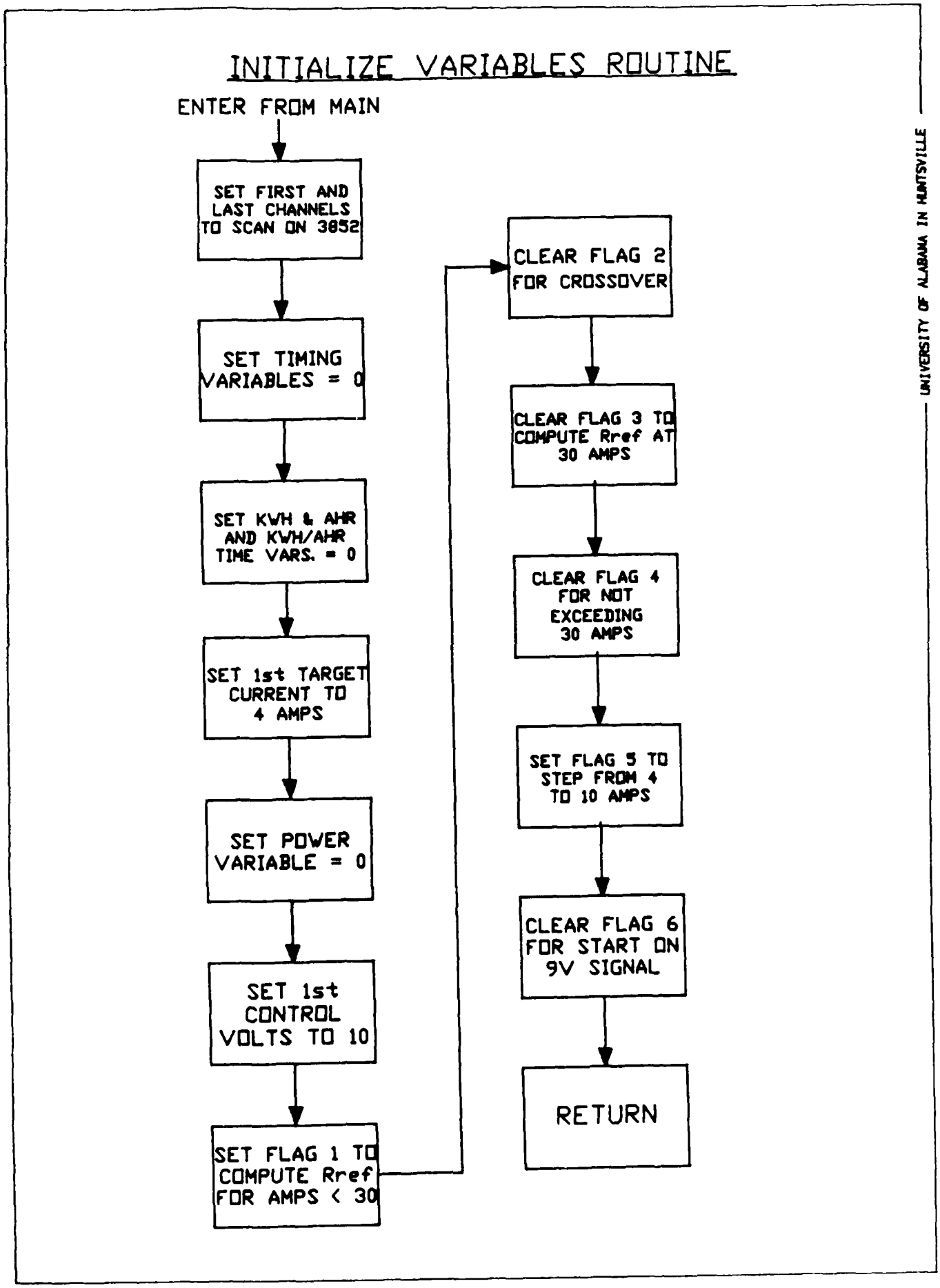

INCREMENT TIMERS ROUTINE

ENTER FROM CYCLE ON INTERNAL TIMER

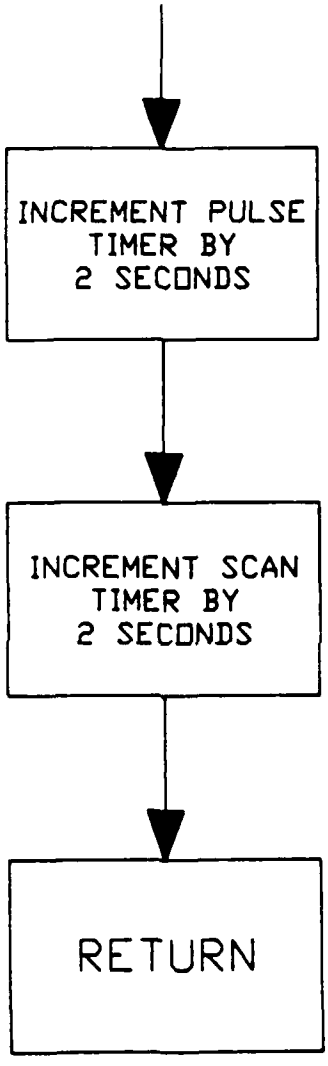

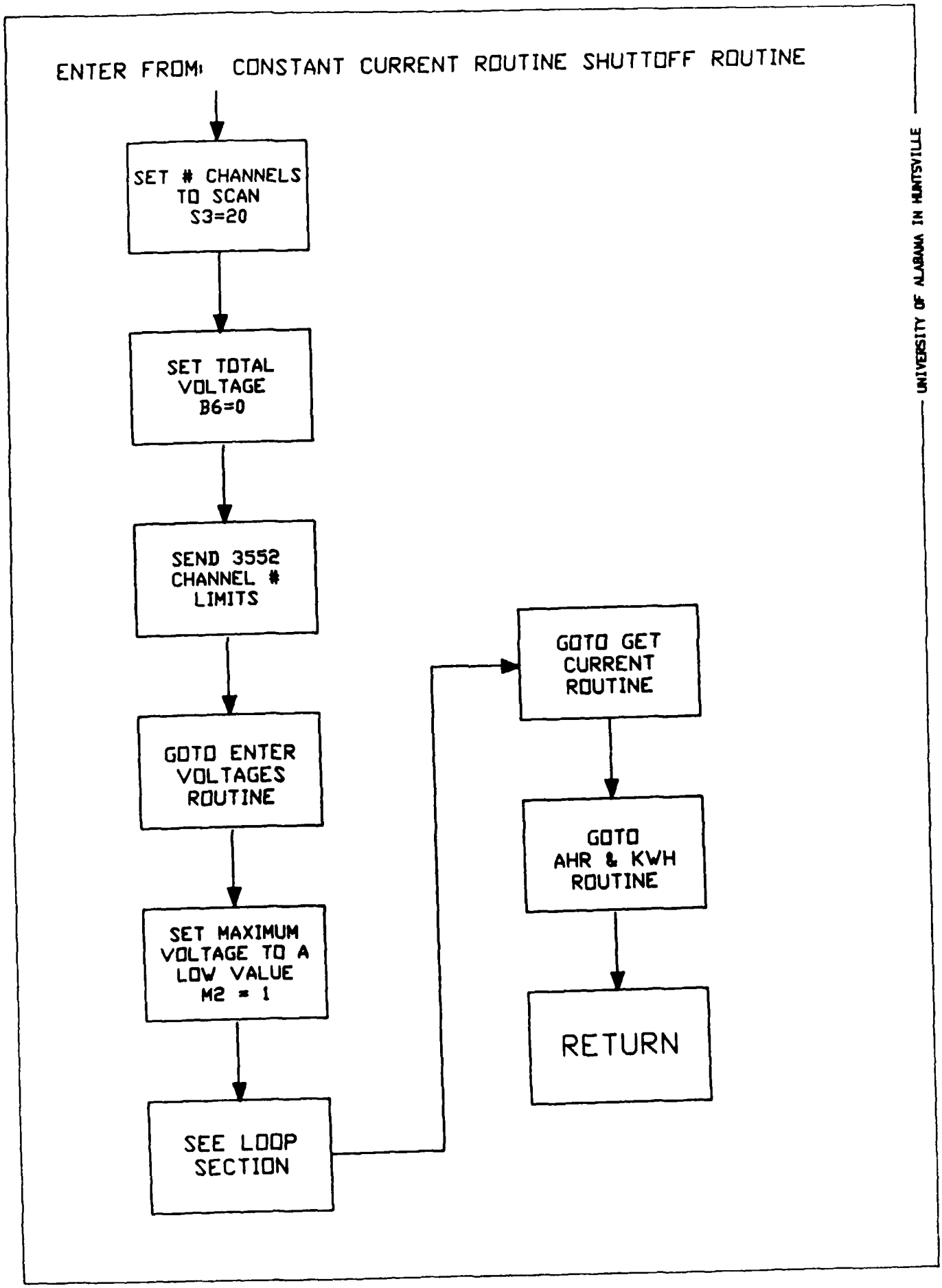
ENTER FROM: CONSTANT CURRENT ROUTINE SHUTTOFF ROUTINE
SET # CHANNELS TO SCAN S3=20
SET TOTAL VOLTAGE B6=0
SEND 3552 CHANNEL # LIMITS
GOTO ENTER VOLTAGES ROUTINE
SET MAXIMUM VOLTAGE TO A LOW VALUE M2 = 1
SEE LOOP SECTION
GOTO GET CURRENT ROUTINE
GOTO AHR & KWH ROUTINE
RETURN
UNIVERSITY OF ALABAMA IN HUNTSVILLE

LOOP SECTION

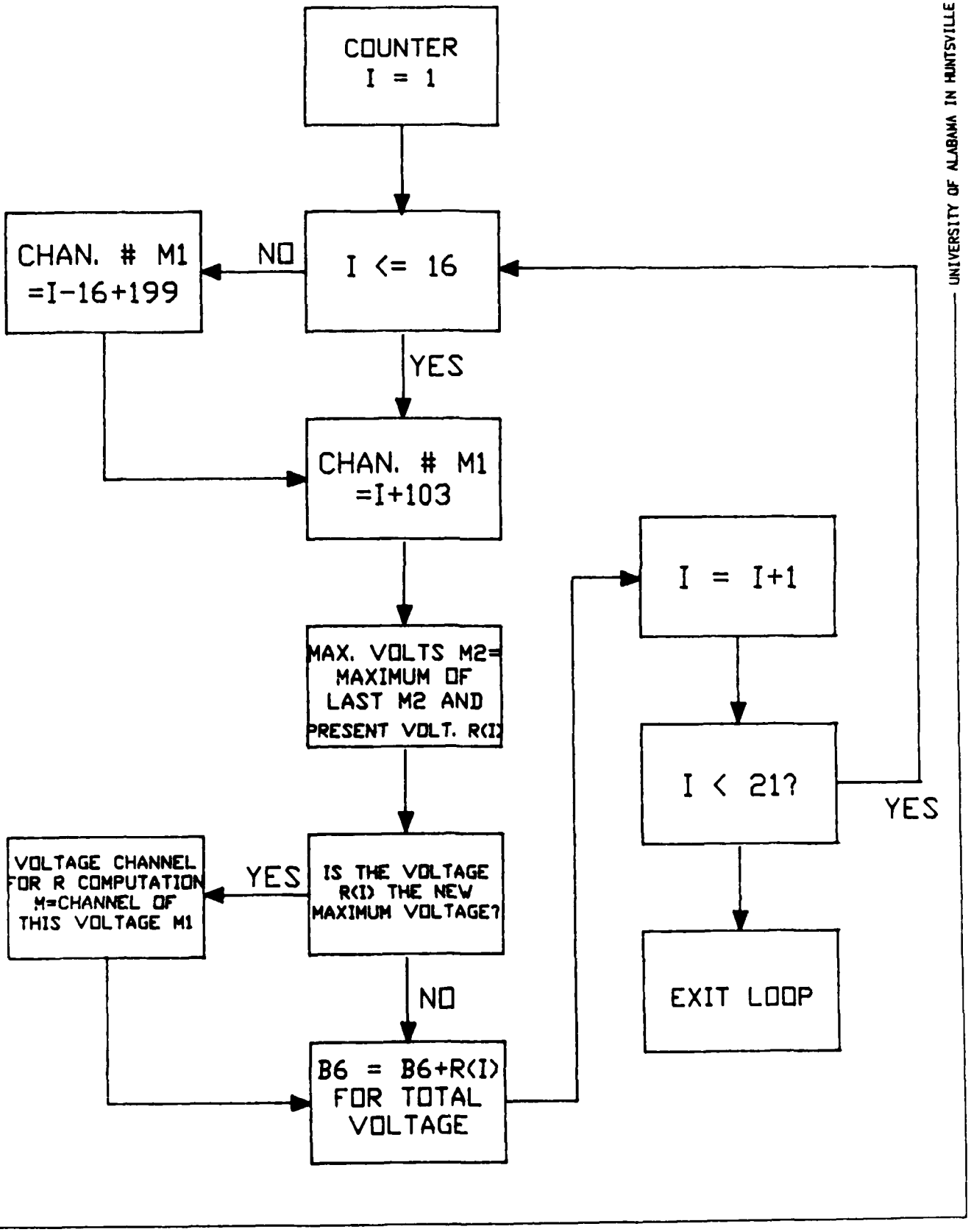

UNIVERSITY OF ALABAMA IN HUNTSVILLE

GET CURRENT ROUTINE

ENTER FROM SCAN ROUTINE

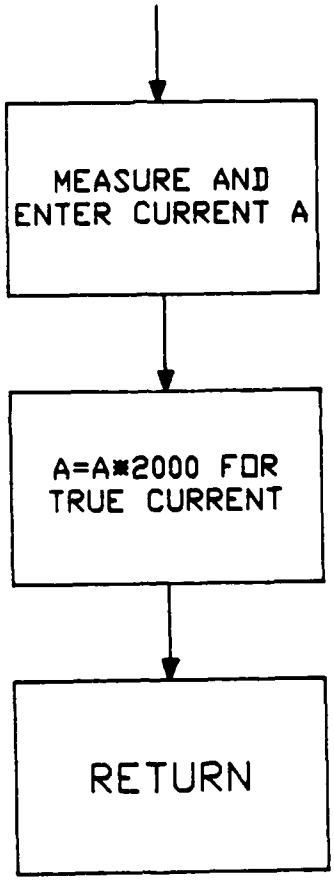

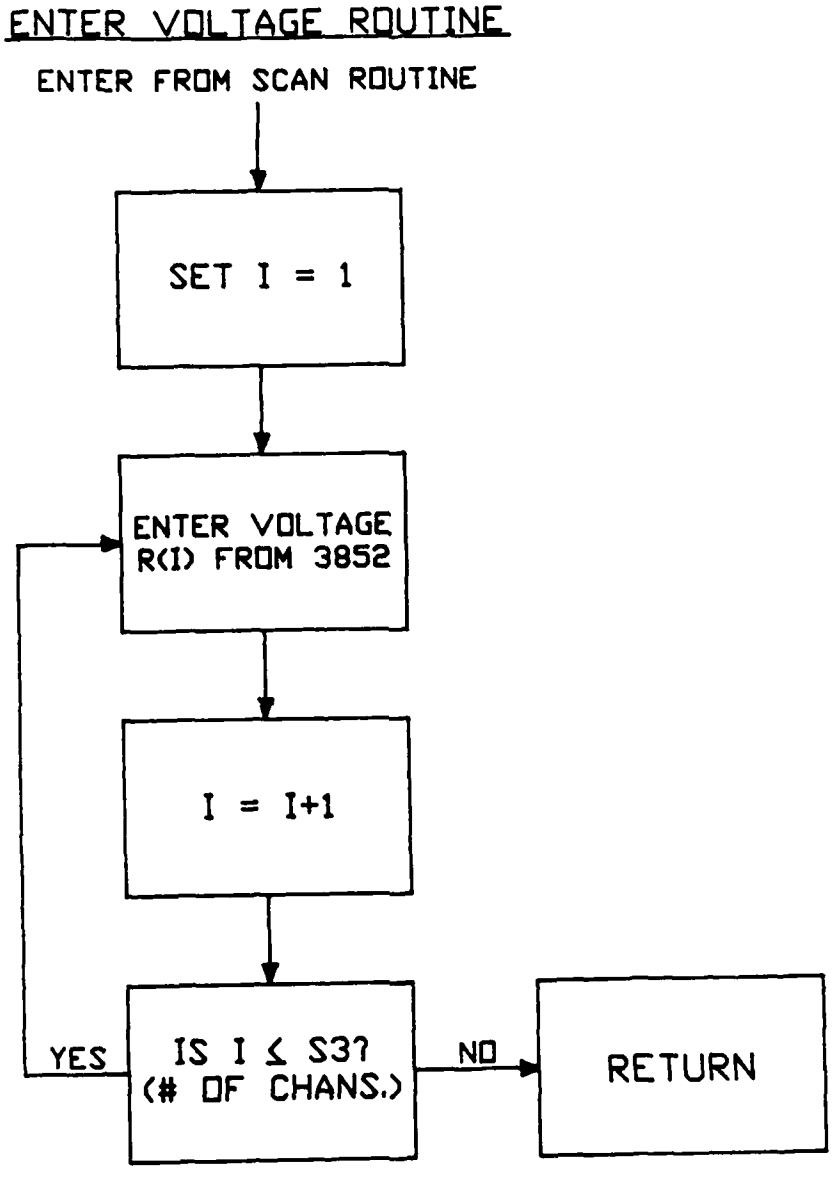
ENTER VOLTAGE ROUTINE
ENTER FROM SCAN ROUTINE
SET I = 1
ENTER VOLTAGE R(I) FROM 3852
I = I+1
IS I ≤ S3? (# OF CHANS.)
YES
NO
RETURN

DATA STORE ROUTINE

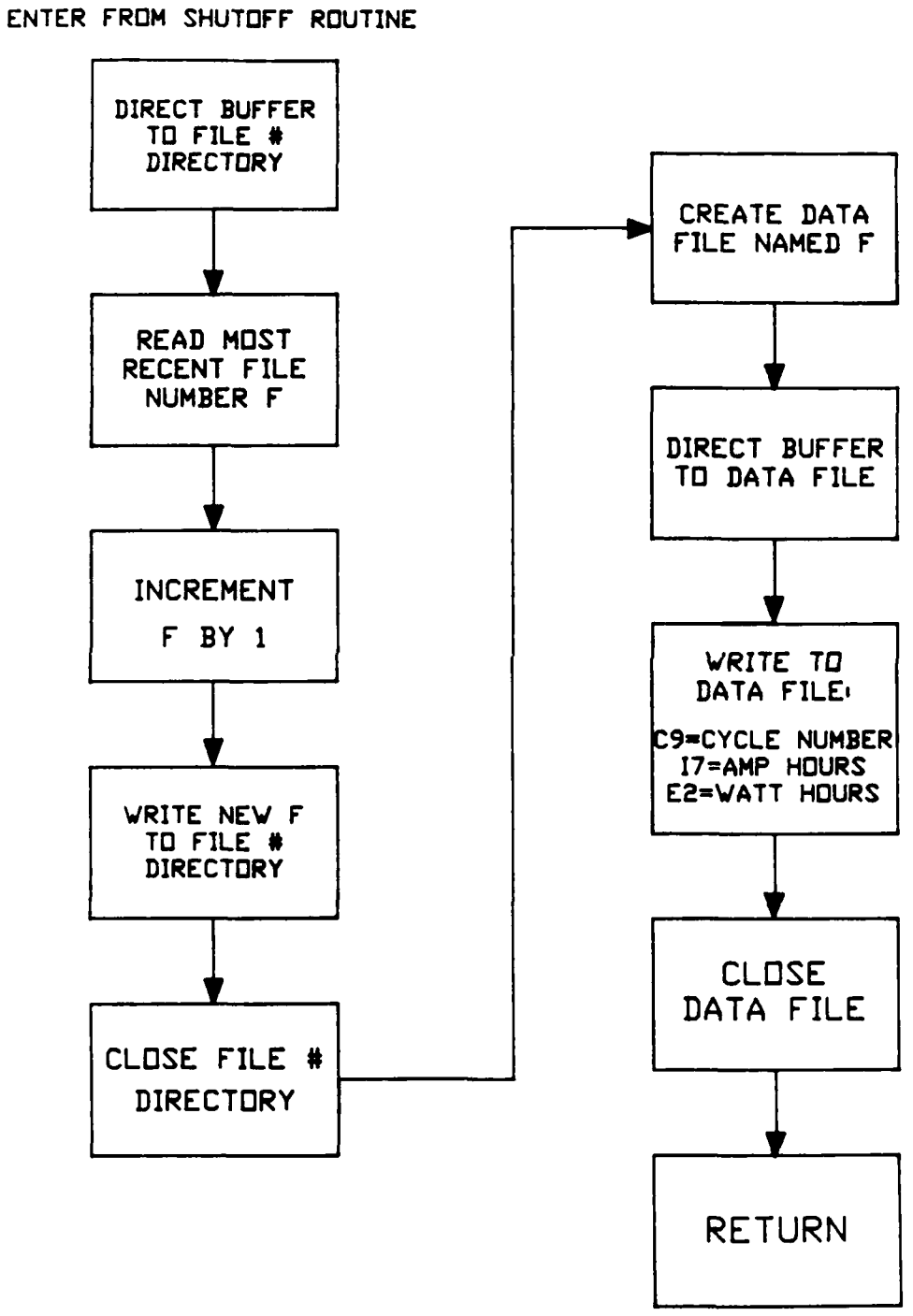

PRINT FINAL DATA ROUTINE

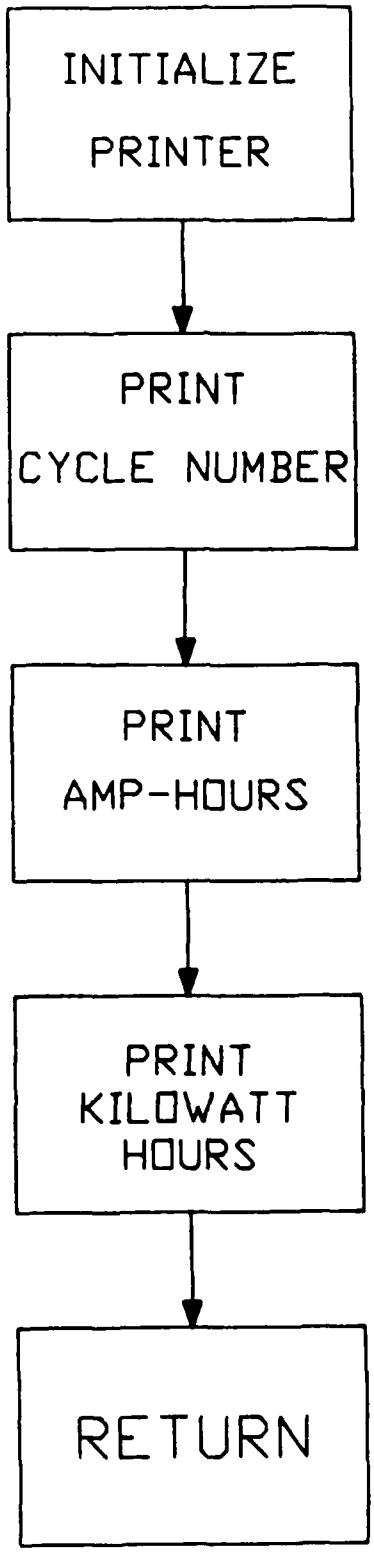

AHR and KWH ROUTINE

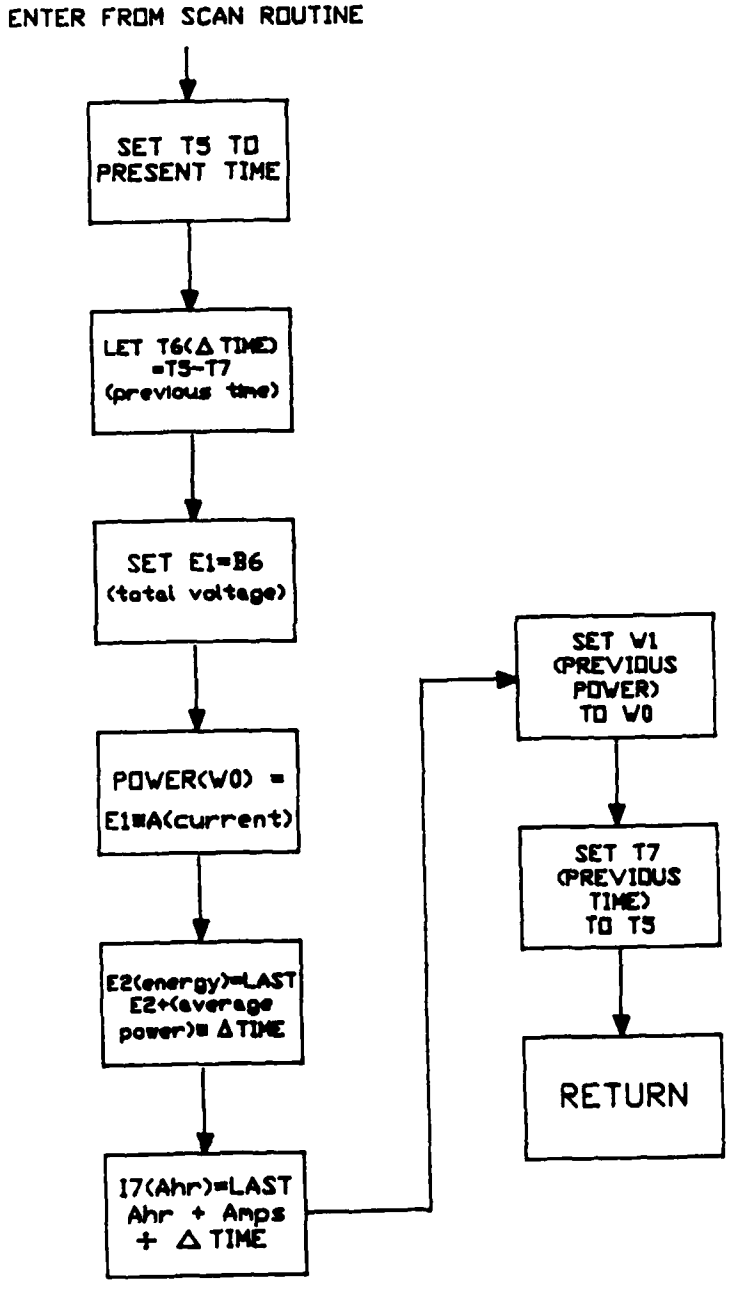

CHARGER OFF SIGNAL ROUTINE

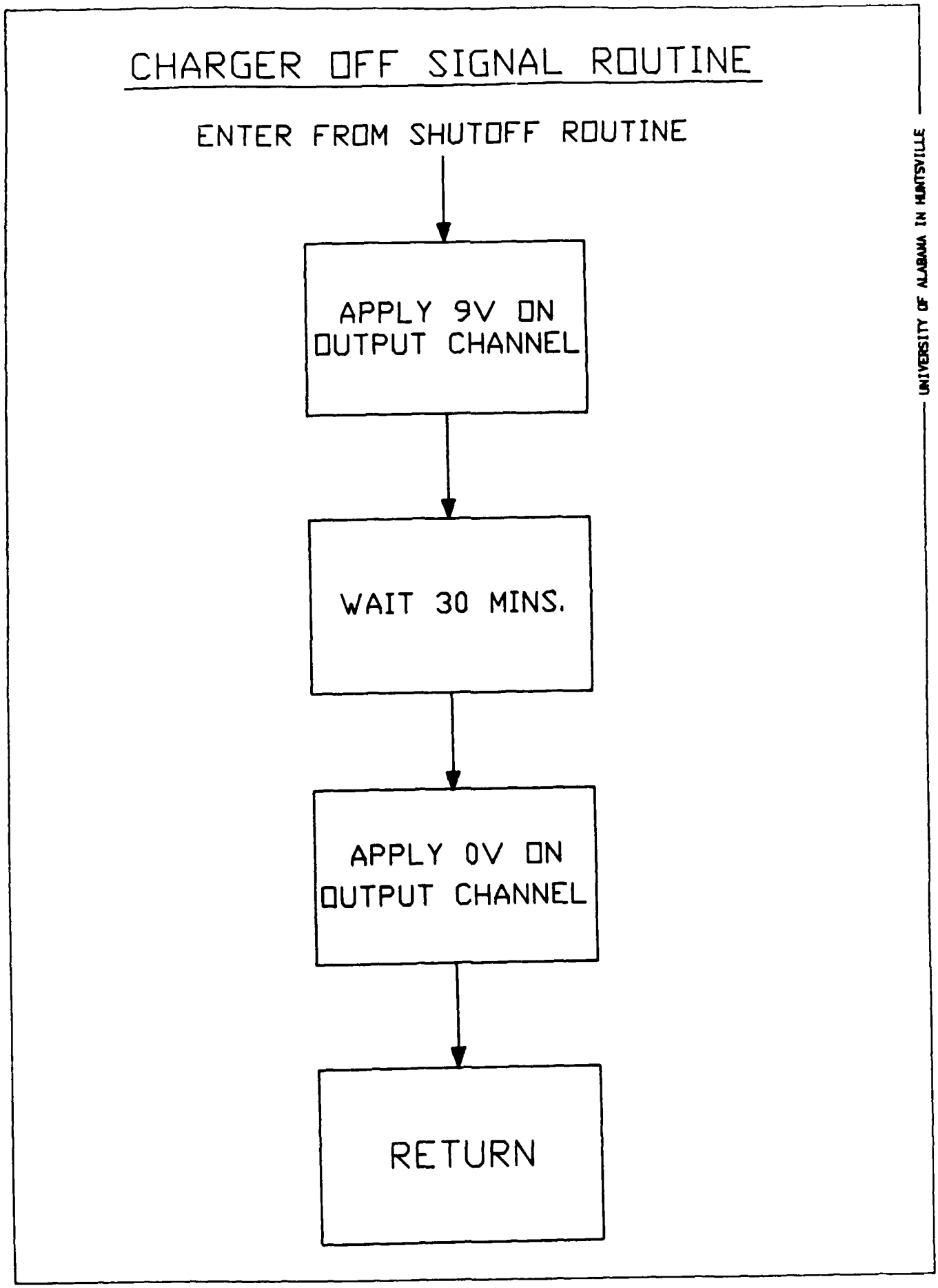

WAIT FOR SIGNAL ROUTINE

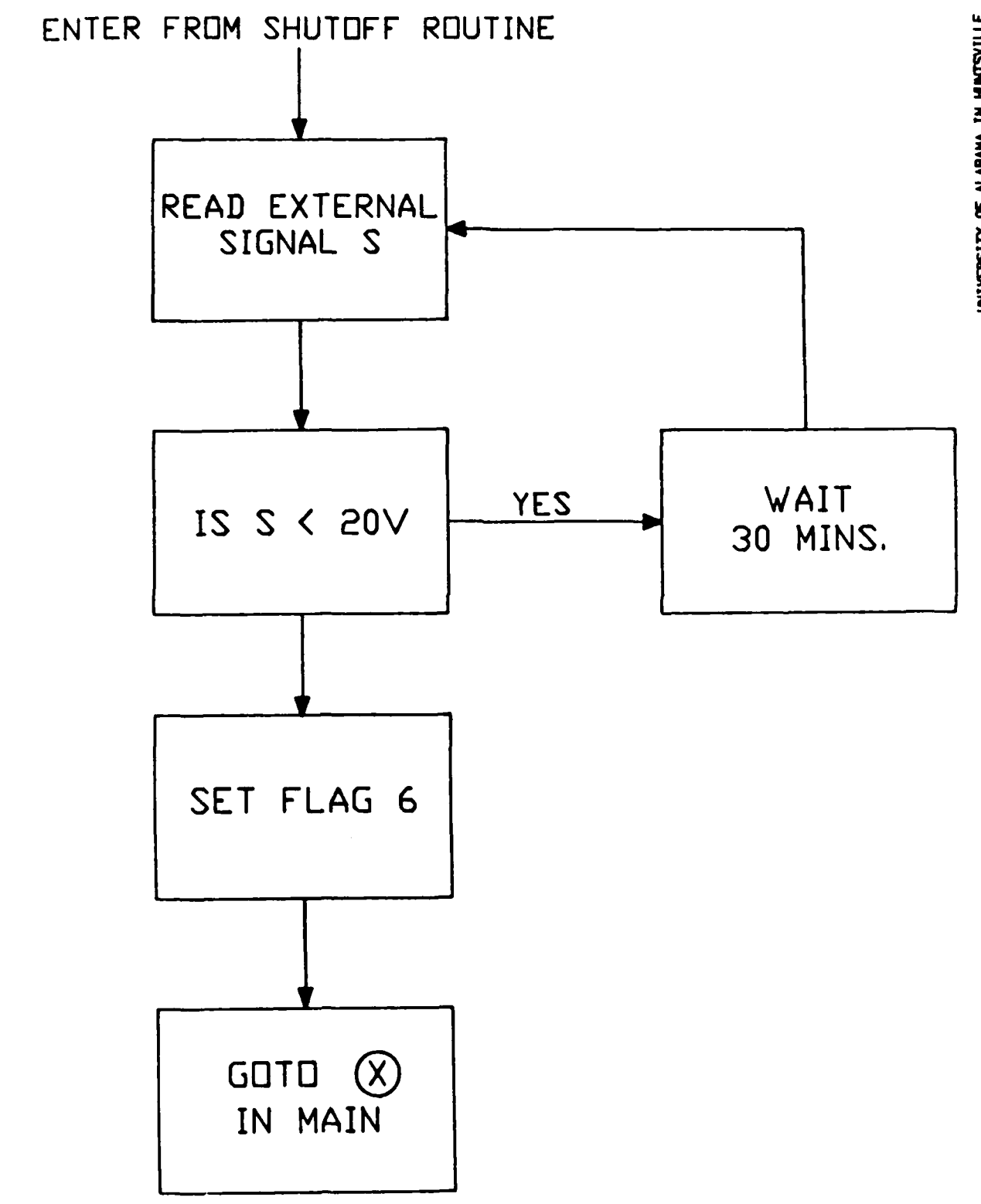

APPENDIX 2

HPL BASIC PROGRAM FOR THE HP85F COMPUTER THAT IS EQUIPPED WITH THE LANGUAGE EXTENSION MODULE AND 125K ADDITIONAL MEMORY

```
10 !        -PROG6-
20 ! LOWER CONTROL VOLTAGE UNTIL 1ST GET A SMALL CURRENT
30 ! INCREASE CURRENT TO 4 AMPS, THEN THIS CONTROL VOLTS-CONT. VOLTS FOR 1ST CU
RENT IS  V
40 ! SCAN 20 VOLTS FOR HIGHEST MODULE AND BASE R ON THIS MODULE
50 ! PULSE AT CONTROL V FOR 4AMPS +  V; THIS IS Rref IF 30 AMPS IS NEVER REACHE

60 ! ALL PULSES ARE  V*2 ABOVE WHATEVER THE CONTROL VOLTS IS AT THE TIME OF THE
PULSE
70 ! WAIT 2.5 MINUTES, THEN PULSE AGAIN.  IF R>2*Rref, LOWER CURRENT BY .3 AMPS
AND:
80 ! REGULATE AT THIS Rref FOR THE REMAINDER OF THE CHARGE, WITHNO FURTHER CURR
NT INCREASES
90 ! IF R OK, RAISE CURRENT TO 10AMPS, WAIT 2.5 MINS.,THEN PULSE AGAIN
100 ! CHECK R AGAINST Rref, LOWER IF NECESSARY, ELSE CONTINUE W/5A STEP INCREAS

110 ! STOP AT 30 AMPS, SCAN, AND GET NEW Rref BASED ON HIGHEST MODULE VOLTS
120 ! SCAN ALL 20 VOLTAGES EVERY MINUTE, AND BASE R ON THE HIGHEST MODULE AND U
DATE AHR & KWH
130 ! CONT. AT 30 AMPS,PULSING EVERY 2.5 MINS. AND SCANNING FOR HIGH MOD. EVERY
MIN.
140 ! ONCE R>Rref, PULSE AND MEASURE EVERY 10 SEC. INSTEAD OF EVERY 2.5 MINUTES
150 ! STOP CHARGE AT MODULE VOLTS>=7.5 OR CURRENT <=2 AMPS
160 ! TIMING DONE BY TIMING VARIABLES INCREMENTED BY ON TIMER DRIVEN SUBROUTINE
170 ! CYCLE #, AHR, AND KWH STORED AND PRINTED AT END OF CHARGE
180 ! SENDS 9V ANALOG SIGNAL AT END OF CHARGE
190 ! WAITS FOR 24V ANALOG SIGNAL BEFORE BEGINNING CHARGE
200 ! -------Main--------------
210 CLEAR ! clear screen
220 DIM R(20)
230 SHORT R,R1
240 CFLAG 6 ! Clear autostart flag 1st time through only
250 GOSUB 1080 ! Initialize
260 OUTPUT 710 ;"APPLY DCV 702";V ! Make sure generator off
270 IF FLAG (6) THEN C9=C9+1 ELSE DISP "ENTER CYCLE NUMBER" @ INPUT C9
280 PRINTER IS 2
290 OUTPUT 710 ;"DISP OFF" ! 3852 works faster with no display
300 IF FLAG (6) THEN 350 ! No manual start if in autostart
310 ON KEY# 1,"START" GOTO 350
320 ON KEY# 4,"OFF" GOTO 430
330 CLEAR @ KEY LABEL
340 GOTO 340 ! idle loop waiting for 'ON KEY' interrupt
350 GOSUB 520 ! Current Start
360 ON TIMER# 1,1000 GOSUB 1230 ! Update timing variables
370 GOSUB 600 ! Maintain amps
380 GOSUB 740 ! Pulse
390 GOSUB 880 ! Resistance
400 IF NOT FLAG (4) AND NOT FLAG (2) THEN GOSUB 940 ! Amps up
410 GOTO 370 ! repeat
420 END
430 ! -------Shutoff----------
440 OFF TIMER# 1
450 GOSUB 1270 ! last scan
460 V=10 @ OUTPUT 710 ;"APPLY DCV 702";V ! high control voltage to stop diesel o
utput
470 GOSUB 1520 ! store data
480 GOSUB 1730 ! Print data
490 GOSUB 1790 ! send charge off signal
500 GOSUB 1840 ! wait for charge on signal
510 STOP
520 ! -----First Current------
530 SETTIME 0,0 ! Set system timer to start of charge
540 OUTPUT 710 ;"APPLY DCV 702";V
```

```
550 OUTPUT 710 ;"CONFMEAS DCV 217"
560 ENTER 710 ; I
570 IF I<.0005 THEN V=V-.005 @ GOTO 540 ! look for 1st availablecurrent
580 C1=V ! control voltage for 1st current
590 RETURN
600 ! ----Constant Current-----
610 IF NOT FLAG (2) AND D1>300 THEN 720 ! pulse every 2.5 mins. before C/O
620 IF FLAG (2) AND D1>20 THEN 720 ! pulse every 10 sec. after C/O
630 IF D2>120 THEN D2=0 @ GOSUB 1270 ! scan
640 OUTPUT 710 ;"APPLY DCV 702";V ! apply control voltage
650 OUTPUT 710 ;"CONFMEAS DCV 217" ! measure current
660 ENTER 710 ; I1
670 IF I1<W-.00005 THEN V=V-.0025 @ GOTO 610
680 IF I1>W+.00005 THEN V=V+.0025 @ GOTO 610 ! raise or lower control V dependi
g on current
690 IF FLAG (1) THEN C2=V @ C3=(C2-C1)*2 @ D1=0 @ D2=0 @ GOSUB 1270 @ GOSUB 740
@ GOSUB 880 ! scan
700 IF FLAG (3) THEN GOSUB 1270 @ GOSUB 740 @ GOSUB 880 @ CFLAG 3 ! get new Rre
 for 30 amps
710 GOTO 610 ! repeat this rou- tine until time to pulse
720 D1=0 ! reset pulse timer
730 RETURN
740 ! ----Apply Pulse---------
750 OUTPUT 710 ;"CONFMEAS DCV,";M ! use highest mod. for R
760 ENTER 710 ; U1 ! voltage be-fore additional current
770 IF U1>= 7.5 THEN GOTO 430 ! shutoff for high mod. voltage
780 OUTPUT 710 ;"CONFMEAS DCV 217"
790 ENTER 710 ; I1 ! prevailing current
800 OUTPUT 710 ;"APPLY DCV 702";V+C3 ! add pulse value
810 WAIT 1000 ! let voltage sta-bilize
820 OUTPUT 710 ;"CONFMEAS DCV,";M
830 ENTER 710 ; U2 ! voltage after additional current
840 OUTPUT 710 ;"CONFMEAS DCV 217"
850 ENTER 710 ; I2 ! new curr.
860 OUTPUT 710 ;"APPLY DCV 702";V ! return to pre-pulse curr.
870 RETURN
880 ! ---Calculate Resistance--
890 R=(U2-U1)/((I2-I1)*2000)
900 DISP "R",R
910 IF FLAG (1) OR FLAG (3) THEN GOSUB 1050 @ RETURN ! Calculate R1 (Rref)
920 IF R>R1 THEN GOSUB 990 ! lower charge current
930 RETURN
940 ! ---Increase Current-----
950 IF FLAG (5) THEN W=.005 @ CFLAG 5 @ RETURN ! Next step after 4 amps is ;10
mps, not 4+5
960 W=I1+.0025 ! add 5 amps
970 IF W>= .015 THEN W=.015 @ SFLAG 4 @ SFLAG 3 ! stop at 30A and set flag for
ew Rref
980 RETURN
990 ! ----Lower Current------
1000 IF NOT FLAG (2) THEN SFLAG 2 ! crossover flag
1010 BEEP 100,200
1020 W=W-.00015 ! lower by .3A
1030 IF W<= .001 THEN GOTO 430 ! stop charge at 2 amps
1040 RETURN
1050 ! --Calculate Rref--------
1060 R1=R*2 @ PRINT "Rref",R1 @ CFLAG 1
1070 RETURN
1080 ! --Initialize Variables--
```

```
1090 S1=104 @ S2=203 ! scan values beginning & end
1100 D1=0 @ D2=0 ! Timing vars.
1110 E2=0 ! variable for energy
1120 I7=0 ! variable for amphr
1130 T7=0 ! time var. for amp hours and energy
1140 W=.002 ! 4 amps
1150 W1=0 ! var. for power
1160 V=10 ! First control volts
1170 SFLAG 1 ! Rref < 30 amps
1180 CFLAG 2 ! Crossover
1190 CFLAG 3 ! Rref for 30 amps
1200 CFLAG 4 ! 30 amps reached
1210 SFLAG 5 ! 10 amp flag
1220 RETURN
1230 ! --Increment Timers-----
1240 D1=D1+2 ! Pulse timer
1250 D2=D2+2 ! Scan timer
1260 RETURN
1270 ! -------Scan-------------
1280 S3=20 ! Number of values to get
1290 B6=0 ! variable for total voltage
1300 OUTPUT 710 ;"MEAS DCV,";S1;"-";S2 ! set 3852 limits
1310 GOSUB 1470 ! data acq.
1320 M2=1 ! low max. at first
1330 FOR I=1 TO 20
1340 IF I<= 16 THEN M1=I+103 ELSE M1=I-16+199 ! channel numbers
1350 M2=MAX (M2,R(I)) ! high mod
1360 IF R(I)>= M2 THEN M=M1 ! highest voltage channel number
1370 B6=B6+R(I)
1380 NEXT I
1390 GOSUB 1420 ! scan amps
1400 GOSUB 1630 ! update amp-hours and energy
1410 RETURN
1420 ! ---Get Current----------
1430 OUTPUT 710 ;"CONFMEAS DCV 217"
1440 ENTER 710 ; A
1450 A=A*2000 ! real current for energy & amphours
1460 RETURN
1470 ! ---Enter Voltages-------
1480 FOR I=1 TO S3
1490 ENTER 710 ; R(I) ! enter voltages
1500 NEXT I
1510 RETURN
1520 ! ----Data Store----------
1530 ASSIGN# 1 TO  "DIR" ! open file number directory
1540 READ# 1,1 ; F ! last file number
1550 F=F+1 @ G$=VAL$ (F) ! tape  file number
1560 PRINT# 1,1 ; F ! write file  number to directory
1570 ASSIGN# 1 TO  * ! close filenumber directory
1580 CREATE G$,3 ! create data file
1590 ASSIGN# 1 TO  G$ ! open datafile
1600 PRINT# 1 ; C9,I7,E2 ! write  cycle#,ahr&energy to data file
1610 ASSIGN# 1 TO  * ! close datafile
1620 RETURN
```

```
1630 ! ---Ahr & Kwh-----------
1640 T5=TIME  ! time
1650 T6=T5-T7 !   time
1660 E1=B6 ! total voltage
1670 W0=E1*A ! power
1680 E2=E2+(W0+W1)/2*(T6/3600) ! energy
1690 I7=I7+A*(T6/3600) ! amp hours
1700 W1=W0 ! previous power for average in energy comp.
1710 T7=T5 ! new previous time
1720 RETURN
1730 ! ---Print Final Data-----
1740 PRINTER IS 2 ! Print to printer
1750 PRINT USING "13A,5X,3D" ; "CYCLE NUMBER:",C9
1760 PRINT USING "10A,8X,3D.2D" ; "AMP HOURS:",I7
1770 PRINT USING "15A,3X,3D.2D" ; "KILOWATT HOURS:",E2
1780 RETURN
1790 ! ---Charger Off Signal--
1800 OUTPUT 710 ;"APPLY DCV 701,9" ! send 9V signal to indicate charge off
1810 WAIT 10000 ! wait 30 mins after sending signal
1820 OUTPUT 710 ;"APPLY DCV 701,0" ! toggle charge off signal to  0 volts
1830 RETURN
1840 ! ----Wait for Signal----
1850 OUTPUT 710 ;"MEAS DCV,207" ! read diesel ready channel
1860 ENTER 710 ; S
1870 IF S<20 THEN WAIT 5000 @ GOTO 1850 ! wait 30 mins. if no start signal, then
 check again
1880 SFLAG 6 @ GOTO 250 ! start cycle on signal
```